MEMO #21

Design considerations for SMA antenna optics

Rachael Padman

2nd July, 1990

Contents

Figure 1: *Basic coordinate system used in this report. Note that the z-axis is directed outwards along boresight.*

Figure 2: *Basic geometry of Cassegrain telescope, showing the notation used in this report.*

1 Basic Geometry

1.1 Coordinate system

At the JCMT we instituted an "antenna-based" (x, y, z) coordinate system, (see Figure 1, which is in fact somewhat counter-intuitive, although it turns out that it is the system which is in general use in antenna engineering. I would suggest that you stick with this, if only to simplify comparison of your results with those appearing in the literature. Note that the z-axis is directed outward from the antenna, along the nominal boresight direction, while the x-axis is vertical when the antenna is pointed at the horizon — that is, for an Alt-Az mount it corresponds to the positive elevation direction. This is the coordinate system adopted in this report.

The basic geometry and notation for the "baseline" Cassegrain system are shown in Figure 2. The following formulae are intended as a ready-reference guide for future work:

1.2 Summary of formulae

The telescope is completely specified by the primary mirror diameter, D, and the primary and secondary focal ratios, F_1 and F_2, or alternatively by D, F_1, and the distance between the prime and Cassegrain foci, $2c$. In this case the primary mirror diameter is set at about 6 m from considerations of field and view and sensitivity; the primary focal ratio is set at 0.42 to match those of the BIMA antennas, and the secondary focal ratio is 10 to give an interfocal distance appropriate to proposed receiver cabin layouts.

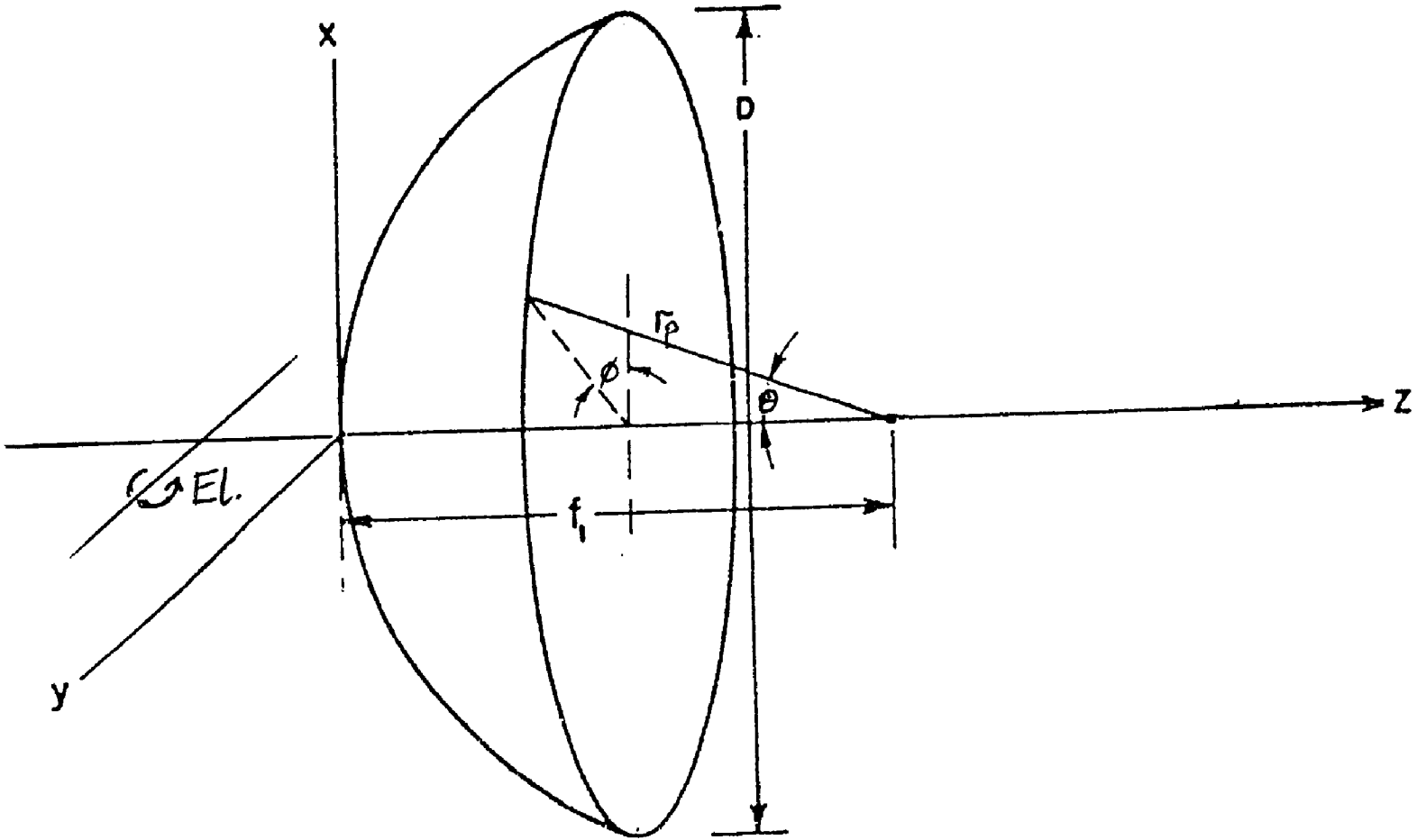
X
D
r_ρ
ϕ
θ
Z
El.
f_1
y

D
θ_e
l_o
D_s
H
2c
l
θ_s

Polar forms

The polar forms for each reflector are quoted for an origin at their respective foci - i.e the primary focus for the primary mirror, and the secondary focus for the secondary mirror.

$$\begin{aligned} r_p &= \frac{2f_1}{1+\cos\theta} \\ r_s &= \frac{(e-1)L_r}{e\cos\theta - 1} \end{aligned} \tag{1}$$

Cartesian forms

The cartesian forms for the two reflectors, in each case based on a point at the vertex of the reflector, and using the (x, y, z) coordinate frame described earlier, are given below:

$$z_p = \frac{1}{4f_1}.(x_p^2 + y_p^2) \tag{2}$$

$$z_s = a[\sqrt{1 + (x_s^2 + y_s^2)/b^2} - 1] \tag{3}$$

where :

$$\begin{aligned} a &= (L_r + L_v)/2e = c/e; \\ b &= a\sqrt{e^2 - 1} \end{aligned}$$

Focal ratios, etc

$$F_1 = f_1/D \tag{4}$$

$$f_2 = M f_1 \tag{5}$$

$$F_2 = f_2/D \tag{6}$$

$$\text{Plate scale} = 206265/f_2 \text{ arcsec/mm} \tag{7}$$

Derived parameters

The front and back focal distances, magnification (M), eccentricity (e) and secondary mirror diameter (D_s), are given by:

$$M = F_2/F_1 \tag{8}$$

$$e = \frac{M+1}{M-1} \tag{9}$$

$$L_r = c + a \tag{10}$$
$$L_v = c - a \tag{11}$$
$$D_s = \frac{a(e-1)D/f_1}{M - (D/4f_1)^2} \tag{12}$$

with:

$$\theta_e = \frac{D/(2f_1)}{1 + (D/4f_1)^2} \tag{13}$$
$$\theta_s = \frac{D/(2f_2)}{1 + (D/4f_2)^2} \tag{14}$$

This leads to the following values for the CfA baseline antenna:

$$\begin{aligned} D &= 6000\,\text{mm} \\ f_1 &= 2520\,\text{mm} \\ f_2 &= 60.00\,\text{m} \end{aligned}$$

$$\begin{aligned} F_1 &= 0.42 \\ F_2 &= 10.0 \end{aligned}$$

$$\begin{aligned} L_r &= 4571.35\,\text{mm} \\ L_v &= 123.65\,\text{mm} \\ M &= 23.731 \\ e &= 1.088 \\ a &= 2158.26\,\text{mm} \\ b &= 923.40\,\text{mm} \\ c &= 2347.5\,\text{mm} \\ D_s &= 457.4\,\text{mm} \end{aligned}$$

$$\begin{aligned} \theta_e &= 61.32^\circ. \\ \theta_s &= 2.862^\circ. \end{aligned}$$

$$\text{Platescale} = 3.449''/\text{mm} \tag{15}$$

2 Feed and subreflector motions

This section lists the consequences of small motions of the feed with respect to the nominal focal position, and of the subreflector with respect to its nominal location. The formulae are

mostly derived in references [1-3]. Ruze[1] presents simple forms of the aperture phase errors and losses arising through various aberrations, for a parabolic aperture amplitude distribution parameterized in terms of the value at the edge of the dish. The formulae, as reproduced below, consist of a fixed analytical part multiplied by factors such as ALAD, BPLLD, *etc.*, all of which tend to 1 in the limits of large focal ratios and uniform illumination.

2.1 Feed translation

Prime focus

The primary beam deviation factor, BDF_1, is defined according to:

$$BDF_1 = \frac{\theta_b}{\tan^{-1} d/f_1}, \tag{16}$$

where d is the lateral shift of the feed in the focal plane, and f_1 is the primary mirror focal length as before. The beam deviation factor depends on the aperture illumination, $g(r)$, and may be computed using the form:

$$BDF_n = \frac{\int_0^1 \frac{g(r)r^3}{1+(r/2f_n)^2} dr}{\int_0^1 g(r)r^3 dr}, \tag{17}$$

with r being the normalized mirror radius, $2\sqrt{x^2+y^2}/D$. For typical values of the primary focal ratio BDF_1 is somewhat less than one (*i.e.* 0.7–0.9). Thus:

$$\theta_b = BDF_1 \tan^{-1} d/f_1. \tag{18}$$

The loss in maximum forward gain associated with a lateral shift Δx_f of the feed is given by Ruze[1], as follows:

$$G/G_0 = 1 - \frac{(2\pi \Delta x_s/\lambda)^2}{18(4f_1/D)^6} \times \text{BPLLD}, \tag{19}$$

where BPLLD is the Beam Peak Loss due to Lateral Displacement, and has a value of around 0.4 for most reasonable illumination tapers and primary focal lengths, f_1. Writing the fractional loss, L, as $1 - G/G_0$, we can rearrange this to give:

$$L = \frac{4\pi^2}{18(4f_1/D)^6} \times \text{BPLLD} \times (\Delta x_s/\lambda)^2. \tag{20}$$

Given that the beam throw $\theta_b \simeq \Delta x_s/f_1$, and the nominal beamwidth $\Theta_B = \lambda/D$, then we can rewrite (19) yet again as:

$$L = 5.35\times10^{-4} \frac{1}{(f_1/D)^4} \times \text{BPLLD} \times (\theta/\Theta_B)^2. \tag{21}$$

Note that the loss computed in this way is *coma* loss only: other sources of loss, such as astigmatism, curvature of field, etc are expected to be much smaller at the short focal ratios typical of radiotelescope antennas, but become dominant at much longer f-ratios.

Cassegrain focus

The secondary beam deviation factor, BDF_2, is also defined as in (17), but with the effective focal length, $f_2 = Mf_1$, now replacing f_1. Note that because $r/(2f_2)$ is always much less than 1, BDF_2 approaches 1 very closely for all sensible values of M.

$$\theta_b \simeq \tan^{-1} \frac{d}{Mf_1} \tag{22}$$

As demonstrated by Murphy & Padman[19], the principal aberration in the case of Cassegrain system is curvature of field. This may be calculated from the wave aberration directly, by equating the quadratic term of the aberration function to the additional quadratic phase across the secondary when the feed is translated parallel to the axis. (The more standard representation in terms of the paraxial radii of curvature of the primary and secondary mirrors gives $R_p = f_1(\frac{\rho}{1-\rho})$, where $\rho = r_2/r_1 = b^2/(2af_1)$.) Note that the Petzval surface sketched in [19] is incorrect, in that the sign of the curvature is that appropriate for a Gregorian system rather than a Cassegrain, for which the Petzval surface should be concave toward the secondary mirror.

Since astigmatic losses are negligible (see [19], appendix 4), the Petzval surface is given by (using the result from the aberration function):

$$\Delta z_f = M\frac{(c+a)^2}{2(F_2 D_s)^3}\,(\Delta x_f)^2. \tag{23}$$

For the CfA antennas this turns out to give a radius of curvature for the Petzval surface of about 200 mm.

For large offsets along the Petzval surface there is an additional *linear* term in the aberration function for the longitudinal component of the motion, which causes a further beam squint of magnitude:

$$\theta_p = \frac{M}{2F_2^3 D_s^2 D}\,(\Delta x_f)^3. \tag{24}$$

This is only relevant in the context of beam-switching, since it is not envisaged that focal plane array detectors will be used on the CfA array antennas. It is clear that for the proposed single detector on-axis the losses due to a fixed feed offset will be negligible once the telescope has been focussed and recollimated (*i.e.* adjusted for the new pointing).

2.2 Secondary mirror translation

Lateral movements of the secondary mirror give rise to pointing offsets equivalent to a combination of feed motions at both secondary and primary foci. Thus:

$$\begin{aligned} \theta_b &= BDF_2\frac{\Delta x_s}{Mf_1} - BDF_1\frac{\Delta x_s}{f_1}, \\ &= -\frac{\Delta x_s}{f_1}[BDF_2 - \frac{BDF_1}{M}]. \end{aligned} \tag{25}$$

Figure 3: *Loss of gain at λ 1 mm and λ 0.35 mm as a function of lateral position of the secondary mirror. This plots only the Ruze gain, with the pointing corrected to place the peak of the beam on the far-field (point) source.*

The dependence of the gain on the subreflector translation has been evaluated numerically for wavelengths of 1 mm and 0.35 mm, and is plotted in Figure (3). It can be seen that to a good approximation the gain loss follows the law $L = .048(\Delta x_s/\lambda)^2$.

2.3 Secondary mirror rotation

Secondary mirror rotations about any axis perpendicular to boresight ("tilts") also give rise to a beam shift and consequent losses. Tilts about prime focus are the easiest to handle, while tilts about other points on the axis can be treated as a combination of a tilt about the focus and a compensating transverse shift. For a rotation angle α in the sense that the mirror moves *up* (away from the primary) on the positive x-axis, the consequent beam shift is given by:

$$\theta = -\alpha(\frac{c-a}{f_1})(BDF_1 + BDF_2). \tag{26}$$

The simple Ruze theory[1] predicts negligible (coma) losses for such a tilt: Nonetheless, as shown in [4], there is a predominately astigmatic term that rapidly renders the losses unacceptable. In the absence of a simple first order calculation I have calculated this term numerically: it seems to depend (very closely) on:

$$\Delta l = \frac{Mc\alpha^2}{(2f_2/D)^2}, \tag{27}$$

where Δl is the maximum path error at the edge of the main dish (the maximum error occurs in the plane of the tilt, and is approximately zero in the other principal plane). Again the loss depends on how centrally weighted the illumination is (phase errors are smallest in the centre of the antenna, where the illumination function is greatest). Figure 4 shows the loss of gain *vs* tilt α for the CfA baseline antennas with 10 dB edge taper. Note that at even the shortest wavelengths the astigmatic gain losses are negligible ($< 1\%$) for subreflector rotations of less than 0.7°, corresponding to a beam throw of $197''$. However at this throw the *total* loss in efficiency is in fact 2.1%, due to vignetting by the tilted secondary mirror and additional spillover losses on the primary mirror; since these are wavelength independent they constitute the limiting factor to the possible beam throw at *long* wavelengths. Note also that the Ruze-type losses rapidly get worse as the center of rotation moves away from prime focus.

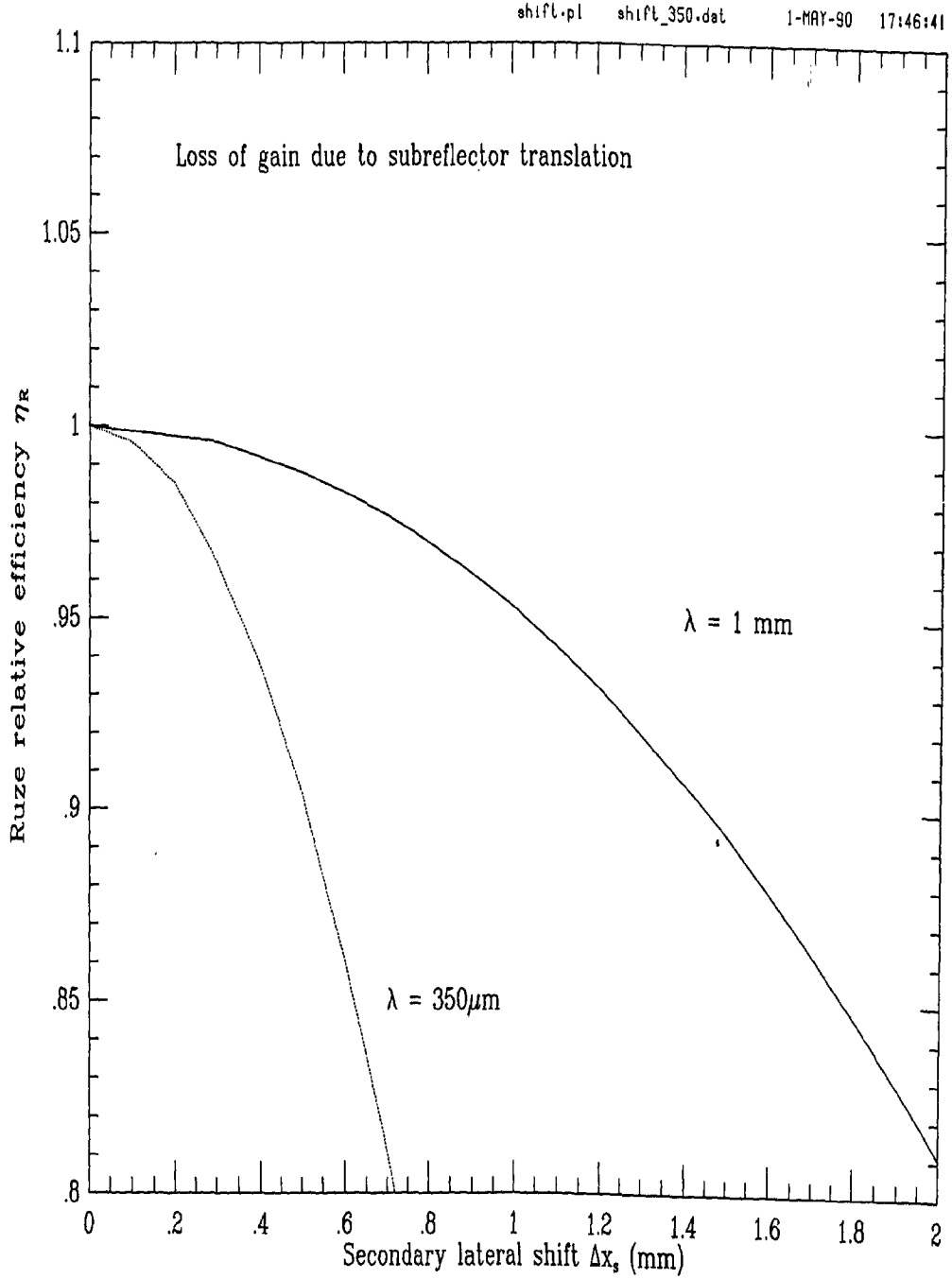
shift.pl shift_350.dat 1-MAY-90 17:46:41
Loss of gain due to subreflector translation
Ruze relative efficiency η_R
1.1
1.05
1
.95
.9
.85
.8
λ = 1 mm
λ = 350μm
0
.2
.4
.6
.8
1
1.2
1.4
1.6
1.8
2
Secondary lateral shift Δx_s (mm)

Figure 4: *Gain loss vs tilt (about prime focus) of the secondary mirror. Both the Ruze gain (i.e. due to astigmatic phase losses only) and the true relative gain are plotted, both for* 10dB *edge taper. The approximately linear loss term is due to spillover and vignetting.*

2.4 Axial defocussing

Axial movement of the feed

Ruze presents a simple formula for the loss due to axial movement of the feed by Δz_f, such that:

$$L = \frac{G_0 - G}{G_0} = \frac{(2\pi \Delta z_f/\lambda)^2}{3(4f/D)^4} \times \text{ALAD}, \tag{28}$$

where f represents either the focal length of the paraboloid for the prime focus case, or the effective focal length $f_2 = M f_1$ in the Cassegrain case, and ALAD is the factor for Axial Loss due to Axial Displacement as tabulated in [1]: for most practical purposes ALAD may be taken as 0.9 at the secondary focus.

Axial motion of the subreflector

For axial motions of the subreflector, the path error is given to first order as $\Delta l = \Delta z_s[(1 - \cos\theta_p) + (1 - \cos\theta_f)]$, where θ_p and θ_f are the angles to boresight an incident ray from the feed makes with the primary and secondary mirrors respectively. Ruze suggests that the errors can then be calculated to sufficient accuracy by substituting a purely quadratic phase error across the dish with the same rim phase error.

In the notation of [1] then we obtain:

$$\Delta G/G_0 = (\frac{2\pi \Delta z_s}{\lambda})^2 \frac{[(1 - \cos\theta_e) + (1 - \cos\theta_s)]^2}{3(1 - \cos\theta_e)(4f_2/D)^4} \times \text{ALAD}(a, \infty). \tag{29}$$

Here θ_e & θ_s are the edge angles of primary and secondary mirrors, as defined earlier, while $\text{ALAD}(a, \infty)$ is the value of ALAD pertaining to the given illumination edge taper and a purely quadratic phase error (see Figure 1 of [1]). For large values of F_2 this simplifies further to:

$$\Delta G/G_0 \simeq (\frac{2\pi \Delta z_s}{\lambda})^2 \frac{(1 - \cos\theta_e)^2}{12} \times \text{ALAD}(a, \infty). \tag{30}$$

These losses are plotted for the CfA baseline antenna in Figure 5.

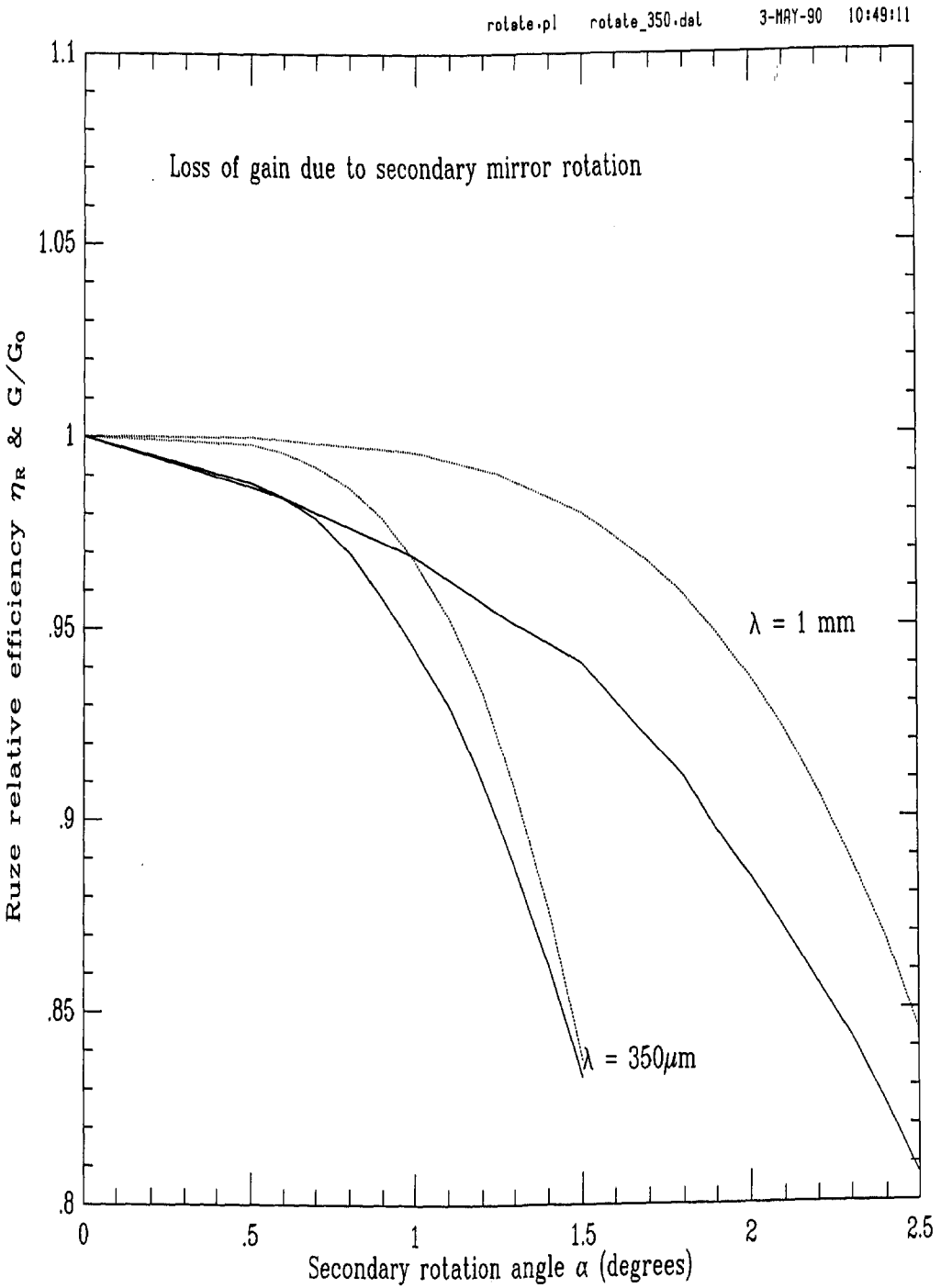
rotate.pl rotate_350.dat 3-MAY-90 10:49:11
Loss of gain due to secondary mirror rotation
Ruze relative efficiency η_R & G/G_o
Secondary rotation angle α (degrees)
λ = 1 mm
λ = 350μm
1.1
1.05
1
.95
.9
.85
.8
0
.5
1
1.5
2
2.5

Figure 5: *Gain losses of the CfA baseline antenna due to an axial shift of the subreflector.*

Refocussing

The ratio of rim path errors resulting from a feed axial shift of Δz_f and from a secondary axial shift of Δz_s is:

$$\begin{aligned}\frac{\Delta l_s}{\Delta l_f} &= \frac{\Delta z_s[(1-\cos\theta_e)+(1-\cos\theta_s)]}{\Delta z_f(1-\cos\theta_s)} \\ &\simeq \frac{2(D/4f_1)^2}{1+(D/4f_1)^2} \Big/ \frac{2(D/4f_2)^2}{1+(D/4f_2)^2} \\ &= M^2 \frac{1}{1+(D/4f_1)^2}. \end{aligned} \tag{31}$$

This results tells us how far it is necessary to move the secondary mirror in order to compensate for an axial offset between the receiver focus and the nominal focus of the telescope.

2.5 Summary of tolerances

Table 1 summarizes the dependence of pointing offsets and gain loss (in the beam peak direction) on the various possible offsets in the telescope geometry: numerical values are given for the dimensions of the "baseline" design, and can be adjusted if necessary using the more detailed information given in §§2.1–2.4.

For reference, for a 10 dB edge taper (equivalent to a value of $a = 0.684$ for parabolic illumination of the form $1-ar^2$ and the same edge taper), and the CfA baseline antenna geometry, I calculate beam deviation factors $BDF_1 = 0.83$ and $BDF_2 \simeq 1.00$. For primary reflector f_1/D of ~ 0.4, values of ALAD and BPLLD can be obtained from figures 1 & 3 of [1] as:

$$\begin{aligned} \text{BPPLD} &\simeq 0.4 \\ \text{ALAD}(0.684, 0.4) &\simeq 0.47 \\ \text{ALAD}(0.684, \infty) &\simeq 0.9 \end{aligned} \tag{32}$$

3 Cross-polarization performance

Cross polarization arises through two main mechanisms[5]. First, the polarization vector from the feed will be rotated at each reflection unless it lies either in or orthogonal to the plane of

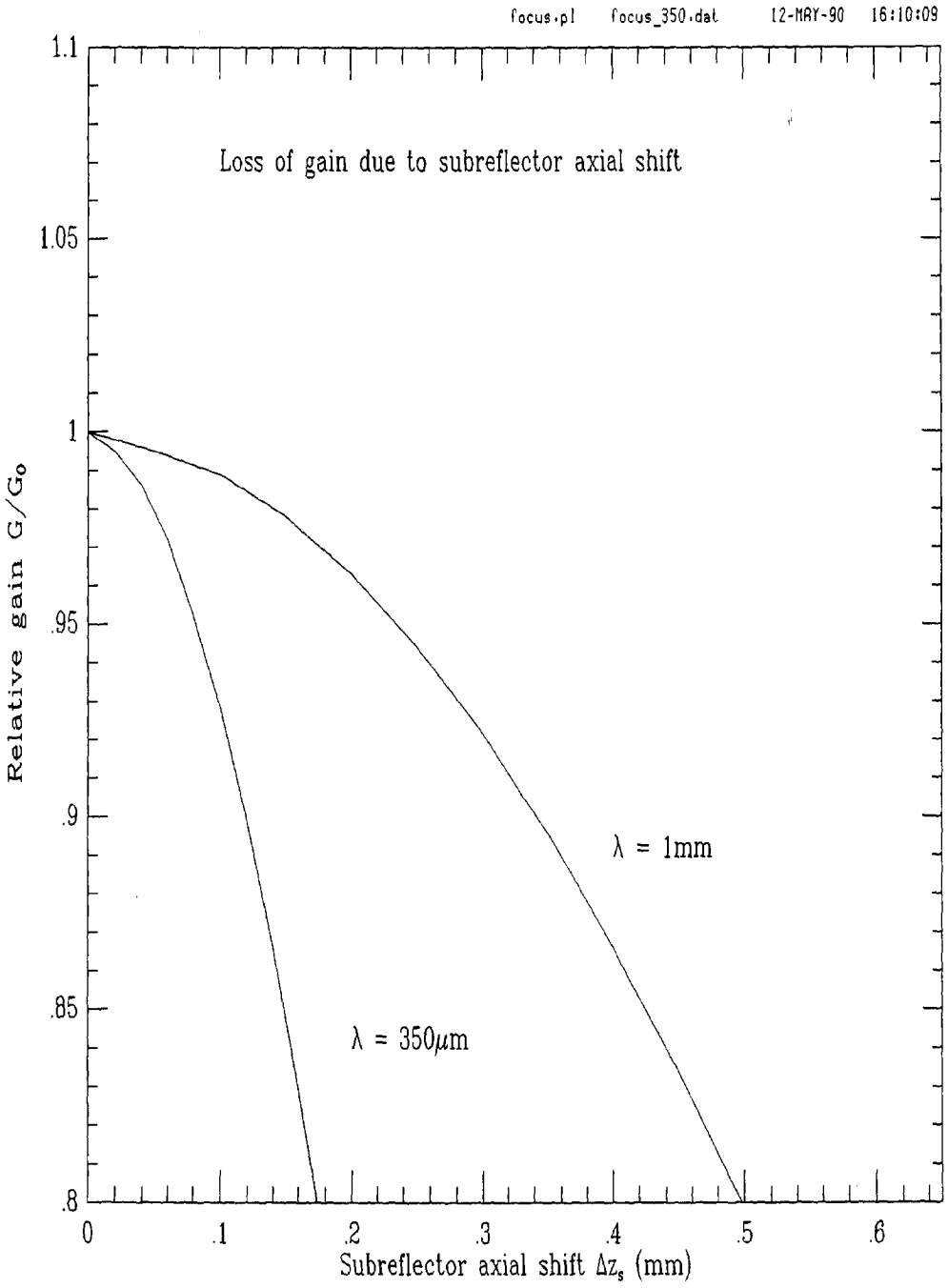
focus.pl focus_350.dat 12-MAY-90 16:10:09
Loss of gain due to subreflector axial shift
Relative gain G/Go
1.1
1.05
1
.95
.9
.85
.8
0
.1
.2
.3
.4
.5
.6
λ = 1mm
λ = 350μm
Subreflector axial shift Δzs (mm)

Parameter	Beamshift factor (arcsec./ mm)	Relative loss $1-\eta_{Ruze}$	Value for 1% loss
Δx_f (prime)	-68.0	$.039\,(\Delta x_f/\lambda)^2$	0.51λ
Δx_f (Cass.)	-3.44	(see text)	–
Δx_s	-64.5	$.048\,(\Delta x_s/\lambda)^2$	0.45λ
Δz_f (Cass.)	–	$5.1\times10^{-6}\,(\Delta z_f/\lambda)^2$	44λ
Δz_s	–	$0.80\,(\Delta z_s/\lambda)^2$	0.11λ

Table 1: *Beamshifts resulting from small offsets in the antenna geometry, and permissible variations for 1% loss of gain in the beam peak direction, all calculated for the CfA "baseline" antenna design discussed in §1. Note that dimensions are assumed to be in millimetres.*

incidence. For a general feed polarization pattern therefore the final aperture fields of even a symmetric antenna will *not* be pure polarized. The second effect is of less importance for large antennas, and arises because of the curvature of the reflector surface: it can be ignored for reflectors with $D/\lambda > 1000$.

The rotation of the polarization vector can be adequately modelled using the methods of Geometric Optics. It is intuitively obvious that for any bilaterally symmetric feed pattern (such as that due to a rectangular or conical horn antenna) the components of the on-axis cross-polarized field due to depolarization in the individual 90° quadrants of the antenna must cancel, and that there will therefore be zero cross polarized response in the boresight direction, or indeed along either of the two principal planes of symmetry (even a circularly symmetric feed pattern has one symmetry plane imposed by the instantaneous feed polarization). The cross polarized pattern must therefore be 4-lobed, and the maximum response generally occurs at about one diffraction beamwidth from the axis, peaking in the $\pm45°$ planes[6].

For a parabolic antenna fed from its prime focus, or for a classical Cassegrain antenna, the feed polarization required to give zero net cross-polarization in the aperture is identically that of a small plane wave (Huygens) source. The class of corrugated horn antennas known as *scalar feeds* very closely approximates the desired fields in the feed aperture, and is therefore capable of yielding very low overall cross-polarization, even at off-axis angles in the radiation pattern. Note that for the Cassegrain antenna this result is true, even though the cross-polarization of the *secondary* pattern is relatively high.

For non-scalar feeds the cross polarization due to the feed is generally dominant. For example, Thomas[5] shows that for a conventional smooth conical horn (TE_{11} feed) the cross polarization for a front-fed paraboloid is roughly -25 dB (and independent of D/λ). Corner-cube antennas will probably generate even higher levels of cross-polarization due to the lack of circular symmetry in their radiation patterns, although they should still have zero *on-axis* cross-polarization due to the existance of a symmetry plane which includes the radiating multipole.

Figure 6: *Aperture illumination function used to examine the effects on cros-polarized sidelobe levels due to blockage by a tripod.*

Program BEAM2 has been adapted to calculate the cross-polar radiation pattern as well as the co-polar pattern, and examples appear in the previous section.

One other concern is that cross-polarization of linearly polarized feed patterns may also manifest itself as a differential beam squint between two orthogonal circularly polarized patterns, as indeed is observed at the VLA[7]. This effect arises because the rotation of the polarization on reflection is indistinguishable from a phase-shift. If the rotation is not identical across the reflector therefore the first order effect is a phase *gradient* which gives rise to a pointing offset. The rotation angle is independent of the hand of polarization, and thus gives rise to equal and opposite phase shifts, and hence beam squints, in the two polarizations[8]. It can be seen that a necessary condition for the first-order term to be non-zero is that the paraboloid be fed off-axis (as at the VLA); for antennas with nominally on-axis feeds this effect should be negligible for all likely offsets. For a prime focus system a rough formula, and further references, are quoted in [20], p147:

$$\sin \Delta\theta = \frac{\lambda}{4\pi F_2 D} \sin \theta_0, \tag{33}$$

where θ_0 is the angle between the feed axis and the antenna axis of symmetry.

I have also investigated (but not in depth) the geometrical optics cross-polarization arising from blockage and shadowing by the struts. A tripod subreflector support was simulated by modifying BEAM2 to increase the mesh resolution to 64×64 points across the aperture, and inserting a simple IF statement to set the aperture amplitudes to zero when the point lay with 5° of the nominal position of a tripod leg. Thus, instead of modelling the blockage and shadowing separately I cheated and assumed that any effects would be seen just by removing a simple angular sector. The resulting aperture amplitude distribution is given in Figure (6). Neither the co-polar nor the cross-polar beam patterns show any evidence of the change at the 5% level, and the relative magnitude of the cross-polar peak is not affected, although the amplitudes of the sidelobes may be affected slightly[20]. Of course, by earlier arguments there should still be zero cross polarization in the $\phi = 0, 180$ plane.

This result really points up once again that for illumination by a scalar feed the aperture cross polarization is so low that in fact it is likely that other (vector diffraction) sources of cross polarization will be much more important. The other test polarization patterns (those of small or Hertzian electric and magnetic dipoles) do not give significantly different results when the angle subtended by the subreflector is as small as this, and probably with more realistic (non-scalar) feed patterns the geometric optics effects would become more noticable.

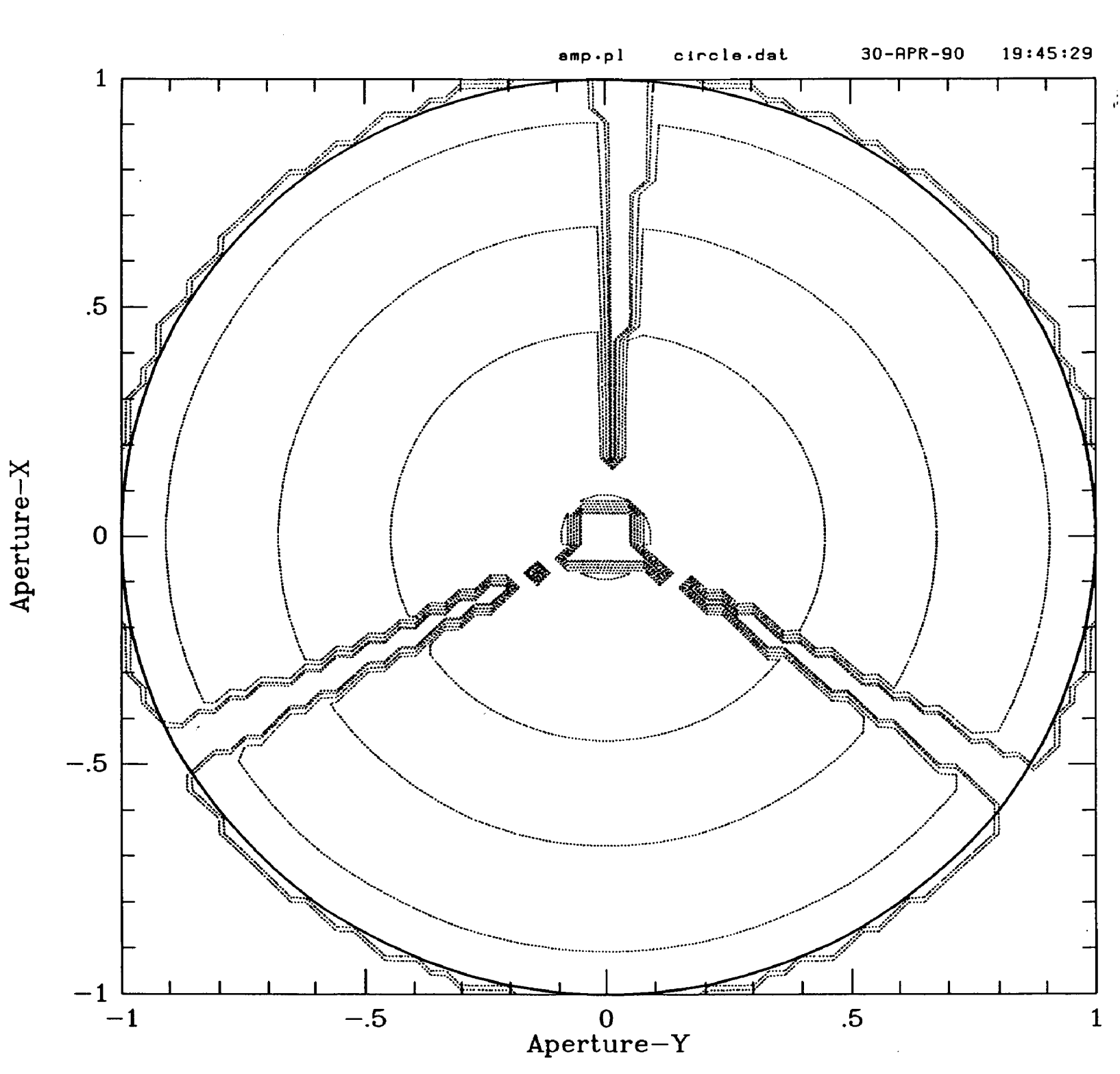
amp.pl circle.dat 30-APR-90 19:45:29
1
.5
0
-.5
-1
-1
-.5
0
.5
1
Aperture-X
Aperture-Y

Figure 7: *Errors arising in Nasmyth transfer mirror system. (a) Due to alignment angle being other than 45°. (b) Due to axial ray not intersecting mirror at intersection of telescope axes. Cases shown are for zenith and nadir pointing; actual errors will be interpolated between these two extremes using* sin(*elevation*).

4 Nasmyth vs Cassegrain focus

This choice only seems to enter the *optical* design in a very limited way. Apart from the overall focal length of the telescope, which is likely to be somewhat longer in most Nasmyth configurations, the only other consideration is that of the tolerances required of the transfer mirror positions and figuring.

At the JCMT we have a single, off-axis, hyperbolic mirror to convert from the $f/12$ incoming beam from the secondary to a $f/35$ beam with a focus on the outside of the elevation bearing. The baseline CfA Nasmyth design calls for two mirrors (see Figure 7), and probably it would be a requirement that at least one of these be flat to avoid having an elevation dependent coupling through the system, although for very small curvatures the losses would be negligible.[10] This would seem to rule out using the extra two mirrors to do any shaping of the illumination (as discussed elsewhere, such common shaped optics are probably too restrictive anyway), but it would be possible to use these mirrors as part of the beamswitch arrangement, *e.g.* as in Figure 9 with one additional mirror so that the arrangement is fed from below.

(18)

Any analysis of the tolerance on the location of the two transfer mirrors will end up looking at three critical parameters — the apparent intersection of the axial ray from the feed with the focal plane (which affects the pointing); the distance by which this ray misses the center of the secondary (which affects the gain); and the variation in the total path with elevation (*i.e.* the antenna phase). Unfortunately, unless the location of the focus can be specified in advance, it is difficult to work these out and present them so that the tradeoffs are immediately obvious.

Some of the basic requirements are fairly simple to see. Considering just the case of two plane mirrors:

- As long as the normals to the mirrors are antiparallel, then the input ray to the "periscope" will be parallel to the output ray.
- The condition on the normals can only be satisfied over a range of elevations if the mirrors are each aligned at 45° to both elevation and azimuth axes. For any other alignment angle an input beam parallel to the azimuth axis will sweep out a cone in space as the elevation changes, and thus the pointing, efficiency and phase will all be affected (see Figure 7a).

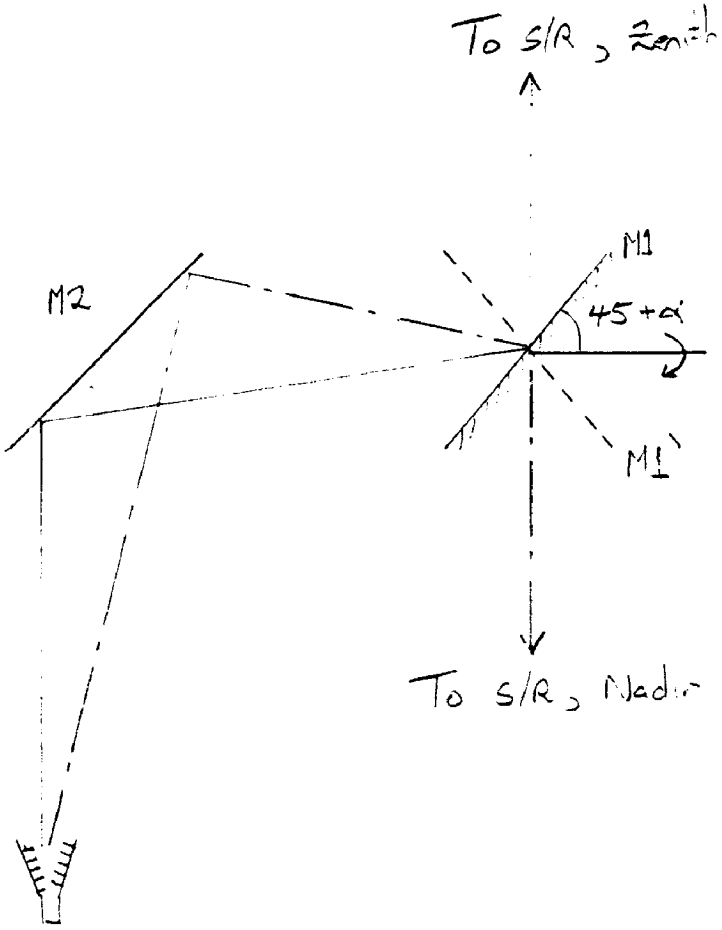
To S/R, Zenith
M1
M2
45+α
M1'
To S/R, Nadir

(a)

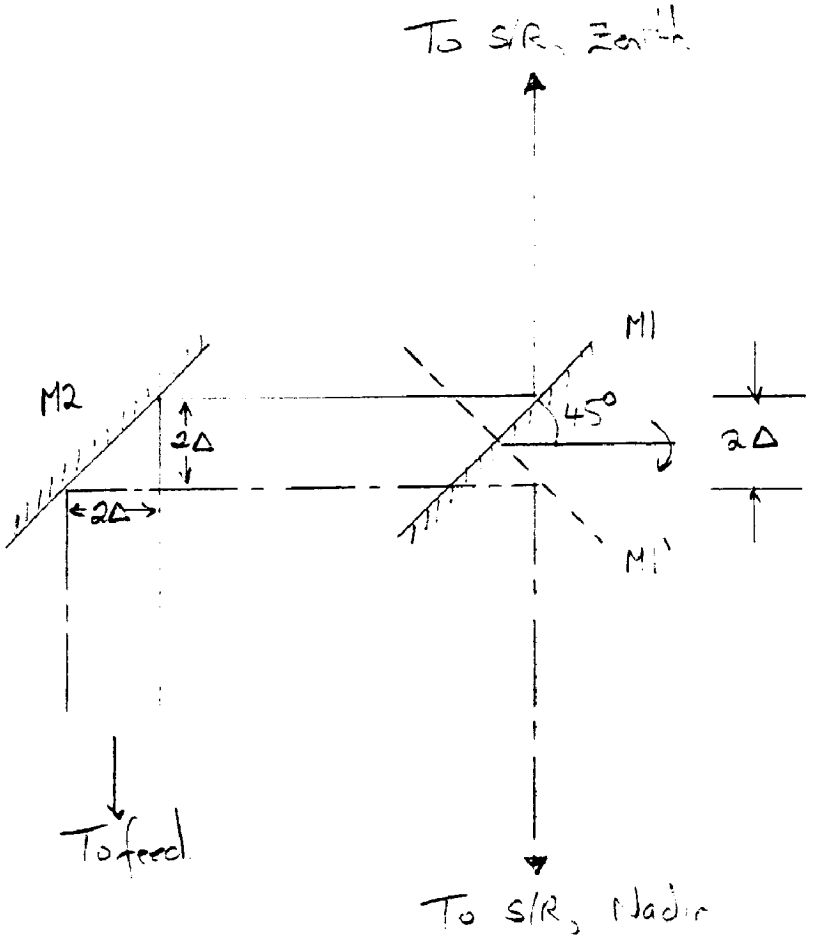
To S/R, Zenith
M1
M2
45°
2Δ
2Δ
2Δ
M1'
To feed
To S/R, Nadir

(b)

Figure 8: *Suggestion for accessing a Coude focus with the same two transfer mirrors required to feed the Nasmyth focus.*

- Unless the axial ray actually intersects the first transfer mirror at the intersection of the two telescope axes, then the ray will describe the surface of a cylinder between the two mirrors, also with an effect on the pointing, but probably less effect on the telescope efficiency and with *no* effect (to first order) on the phase (see Figure 7b).

In terms of setting up the transfer mirrors then, it should be ensured that the mirrors are aligned with respect to both angle, and, less critically, absolute location. It will probably be advisable to include a reference laser beam in the receiver package, which can independently be co-aligned with the radio beam, and to use this for final alignment purposes.

As a final aside here, Richard Hills has pointed out to me that by allowing the telescope to be mounted offset from the azimuth axis, it is possible to feed a *Coude* focus using just the same two mirrors (see Figure 8). Given what I understand to be the difficulties of fitting a Nasmyth cabin between the elevation bearings, and the continuing wish to keep the receivers in a single attitude for reasons of both stability and ease of access, this would seem to be worth serious consideration. The considerations for the transfer mirrors would seem to be identical to those for the Nasmyth option, although it might be necessary to either move to a longer f-ratio or to make one of the mirrors curved in order to achieve a final focus as far down the beam as this. There would however be some additional book-keeping necessary to keep track of the antenna phases, particularly if there is the possibility that the antennas might be positioned in different orientations with respect to the sky.

5 Arrangements in the cabin

5.1 Beamswitch

Basic requirements

It is anticipated that the individual antennas of the SMA may be used in single dish mode, either for pointing checks or to map relatively large scale structure in times of poor interferometer seeing. At submm wavelengths the sky opacity is high and variable, and so some form of rapid switching is required. A chopping secondary mirror has been ruled out on grounds of complexity, as not being required for basic array operation. The choice then narrows to either a *wobbler*, located at an image of the primary mirror, or to a *focal-plane chopper*, located as the name suggests close to the telescope focal plane or an image thereof. Both of these techniques have advantages and disadvantages which must be set against the basic requirements:

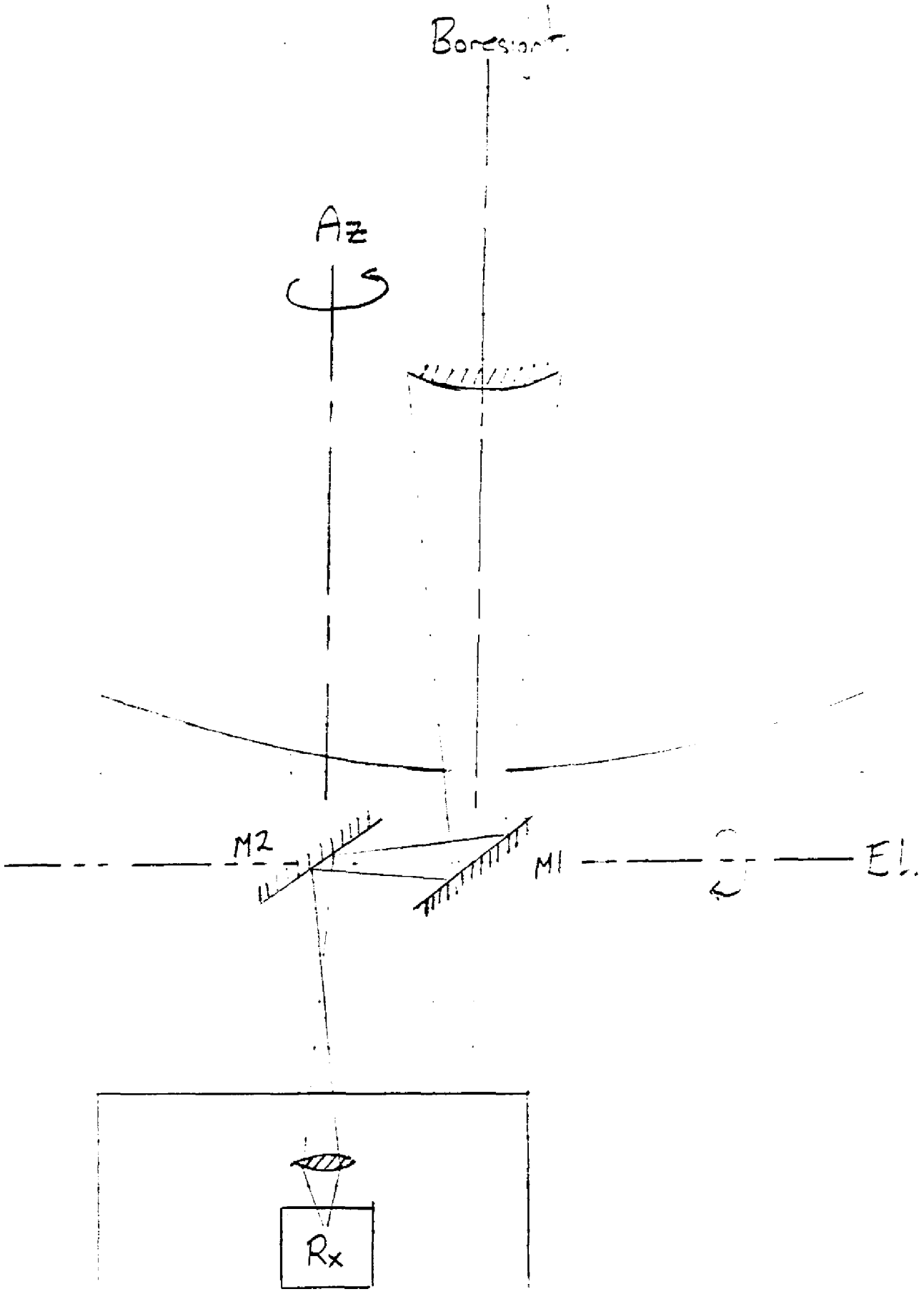
Boresight
Az
M2
M1
El
Rx

Figure 9: *Sketches of various techniques for implementing a focal plane chopper: (a) On-axis main beam chopped against off-axis reference beam; (b) Two beams with identical properties. Note that in both cases the beams are drawn geometrically to emphasize the location of the geometrical foci, but in practice minimum diameters apply to mirrors and stops in the vicinity of the foci, as discussed in the text.*

- Beam throw and direction
- L/R beam symmetry
- Switch frequency
- Pointing and phase degradation

The minimum requirement is probably that we be able to do single-dish pointing and focussing on planets, by switching one high efficiency on-axis beam against blank sky. The maximum beam size, of $\sim 50''$ at 230 GHz is comparable with the angular size of Jupiter, which suggests that a chop amplitude around 5 arcmin will be sufficient. A chop frequency in excess of 10 Hz is desirable, but only enters the optical design insofar as it may be hard to achieve this frequency with a good mark/space ratio if the moving mirror has too large a moment of inertia.

Focal plane beamswitch

The focal-plane beamswitch is fundamentally the easier to implement. There exist a number of configurations in which the "main" beam can be axial and reflect only from fixed mirrors, while the "off" or reference beam is then obtained by inserting a second (movable) mirror in the beam. The simplest such scheme is illustrated in Figure 9(a).

Whilst this scheme achieves the major goals of allowing a rapid switch, with chopping efficiency independent of beam throw, and moreover does not require *any* additional reflecting surfaces, a moment's thought shows that it also has a number of (significant) drawbacks:

- It is not possible to achieve an arbitrarily *small* chopper throw, although for a reasonable thickness chopper blade it may be possible to get this down to something of the order of half a beamwidth or so.
- If the default beam is to be on-axis then there is necessarily an imbalance between the ON and OFF beams. Additional complications (as in Figure 9b) are necessary to allow Left/Right chopped beam symmetry while retaining an axial feed for unchopped observations.

(a)

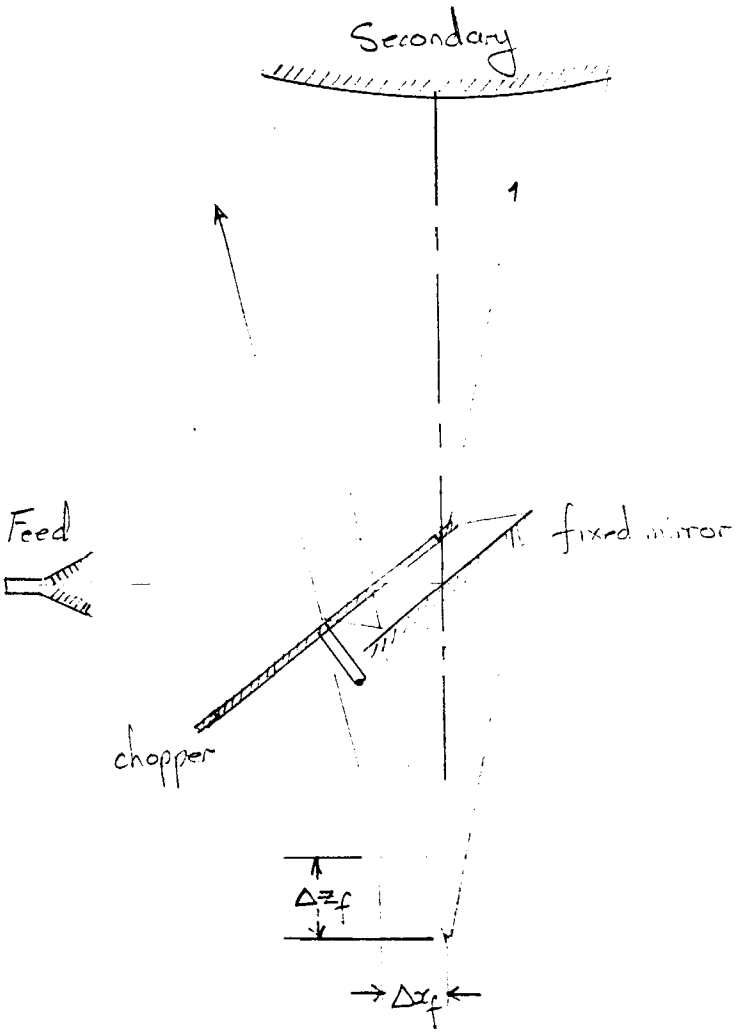
Secondary
1
Feed
fixed mirror
chopper
Δz_f
Δx_f

(b)

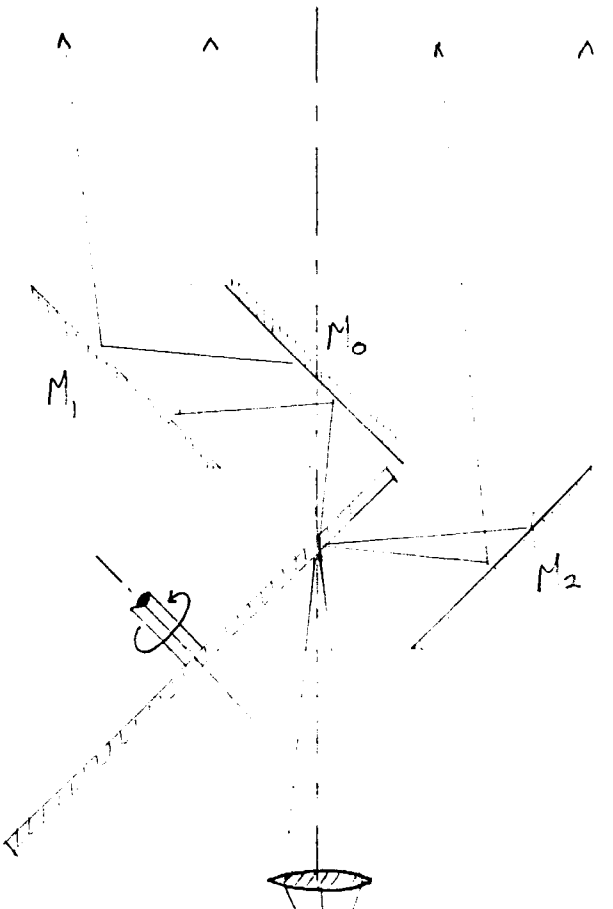
M_0
M_1
M_2

Figure 10: *Sketch of basic optics of an aperture plane wobbler (intended to move the final beam on the sky).*

- It is only easily possible to chop in a single fixed direction unless a complicated turret is built to allow the feed pattern to be injected at arbitrary azimuth.

Aperture plane beamswitch

In comparison with the focal plane chopper, the wobbler is potentially a much more versatile device, pretty much akin to the chopping secondary in effect, and certainly overcomes the disadvantages of the "minimal" chopper described in the previous section. By locating the wobbler at a greatly reduced image of the primary mirror it can be made small enough that rapid switching (with arbitrary throw in an arbitrary direction) is still possible. Against this we also have to set a number of disadvantages:

- Overall the general complexity of the drive mechanics, electronics and software begins to approach that of a chopping secondary mirror (which was thought to be too complicated...).
- It is not easily possible to observe without the wobbler in the system. Thus at least three extra surfaces (see Figure 10) are required, and there is the real possibility of introducing unnecessary additional phase terms if the mirrors cannot be held absolutely fixed for interferometric observing.
- If on the other hand the wobbler is designed as a removable (*i.e.* in-line) device, then even more reflecting surfaces are required when the wobbler *is* in use.

Comparison with chopping subreflector

Both the focal-plane chopper and wobbler are fundamentally equivalent to the chopping secondary, with the exception that in both cases the beam shifts *inside* the telescope structure in the former two cases, but is fixed with respect to the structure in the latter. This implies that it would be advisable to leave somewhat larger beam-clearances (for example where the beam transits the backing structure) when the focal-plane chopper or wobbler is used, to avoid stray "thermal offsets".

As with all chopping mechanisms it is desirable that the moving mirror define the basic exit-pupil of the telescope, to avoid variable spillover in the ON and OFF beams. This must be set against the wish to make maximum use of the antenna aperture in the on-axis case (if

(a)

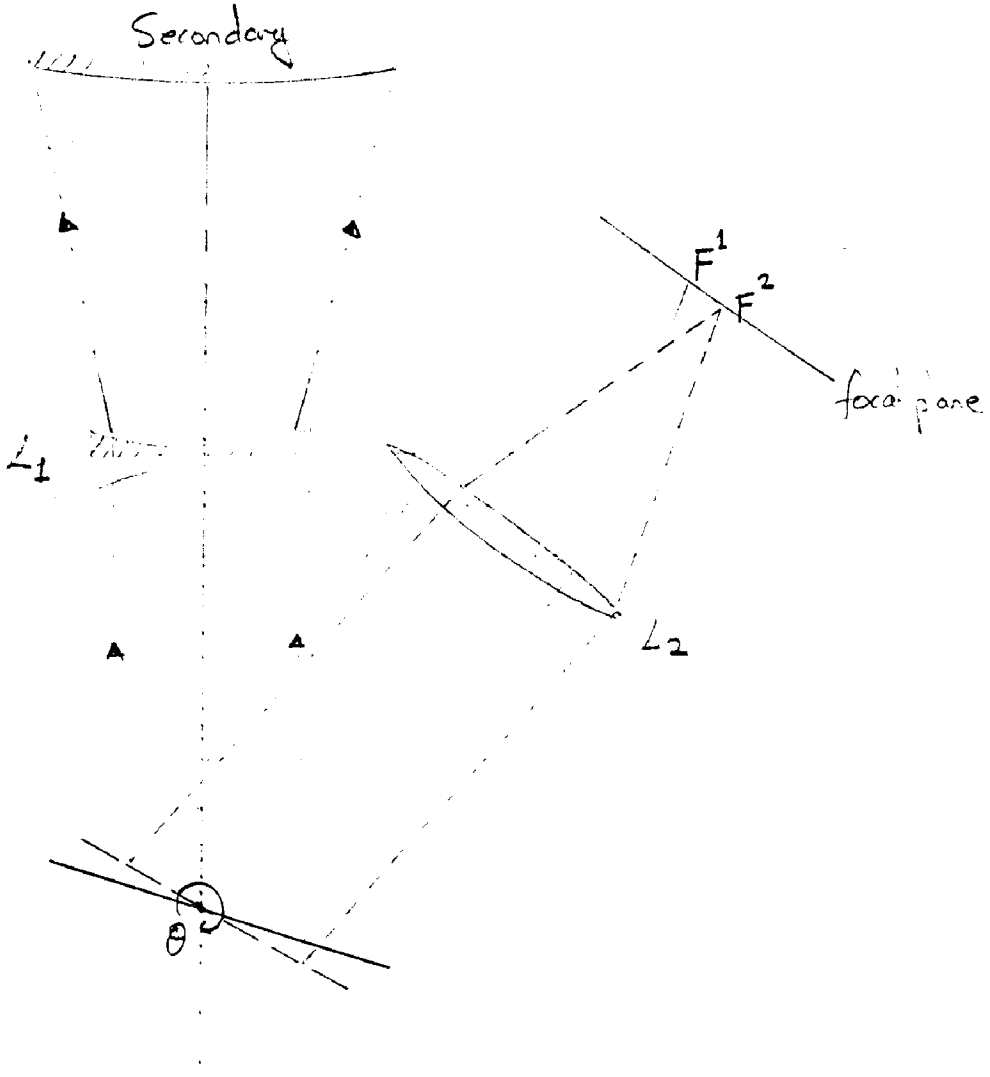

the wobbler say is small enough to give zero geometrical spillover at the extremes of its chop throw, then the primary mirror will be underilluminated in the on-axis case). However this is a problem that is equally applicable to the case of the chopping secondary mirror, and the same compromises need to be made. One possible solution is to add a (cheap!) guard ring to the primary aperture to redirect spillover radiation onto the sky, rather than have it terminated at a probably less stable ambient temperature.

Effect of shaped antenna and/or feed pattern

As shown in [17], when a Cassegrain antenna is perturbed to give higher efficiency, the main effect on the reflector profiles is to reduce the radius of curvature of the secondary mirror. This in turn also increases the Petzval curvature and reduces the useable field (*i.e.* the aberrations for a given off-axis distance increase). Thus with a shaped system the maximum chop throw will be significantly reduced.

With a shaped feed illumination on the other hand, the only effect of the shaping is to give more weight to phase errors in the outer part of the aperture. This also reduces the useable field, but by much less than does the "common" shaping referred to in the previous paragraph. The only thing we need to watch now is that any stops in the focal-plane (e.g the chopper blade in the case of a focal-plane chopper) are made large enough that we still obtain useful chopping efficiency, remembering that the focal-region fields for uniform illumination extend to many "bright rings" of the Airy pattern.

Discussion

It would seem better to use a simple focal-plane chopper, accepting its limitations, than to take on the additional complexity, in terms of both the hardware and software, and the large number of extra reflections, associated with a wobbler. For unshaped reflectors the size of the chop that will still give reasonable ON and OFF beams is determined by the depth of focus and the Petzval curvature, with a small additional term (see [19]) associated with the curvature of the wavefront over the off-axis horn. Assuming this latter term to be negligible, then the maximum allowable chop for (say) 1% error is set primarily by the depth of focus, which as shown in Table 1 is $\sim 44\lambda$, or 15 mm at $\lambda = 0.35$ mm, giving a chop throw of only 53" (this is measured with respect to the Petzval surface, and is essentially independent of the beam offset for all reasonable offsets). The throw can be approximately doubled if we accept that both beams are to be out of focus by the same amount but in opposite directions. As noted elsewhere, if shaped illumination is to be used the focal plane optics (fixed mirror and chopper wheel blades) need to have diameters in excess of 85 mm to achieve efficiencies much greater than 90% overall.

The *size* of the chop throw can be increased either by transforming to a much longer focal ratio (but only at the cost of requiring even larger optics in the focal plane), or by relaxing the requirements such that the symmetry of the ON and OFF beams is lost. This would then

preclude nodding, but might still be acceptable if the main aim of chopping were to subtract out a rapidly varying atmosphere.

Configurations to give a *balanced* chop also exist (*e.g.* see Figure 9b), although they have a number of drawbacks. Assuming that each beam has an associated flat in the focal plane, the minimum chop throw for any reasonable arrangement of mirrors is something in excess of two mirror diameters, or 170 mm $\simeq 600''$ for the shaped feed function. With such an arrangement there are always at least two extra flat mirrors in the beam, and the default beam is off-axis unless the center part of the chopper is made removable. Numerical modelling shows that at a wavelength of 0.35 mm and essentially uniform illumination of the secondary mirror, the total losses amount to about 3.5% in this configuration: 1.5% in phase-errors, and the remainder in spillover. This is probably an overestimate of the losses, since for any realistic feed pattern there must be some edge taper, which will significantly reduce the spillover term, while the phase-errors do not take the Petzval curvature into account properly. Thus this is probably a workable solution, which will give reasonable chop throws at $\lambda = 1.3$ mm and reasonable efficiency at $\lambda = 0.35$ mm.

5.2 Frequency and polarization multiplexing

The basic requirements are for simultaneous operation in at least one polarization at 230 GHz, plus either one or both polarizations at any other frequency. The requirements can be met at the minimum level by using a simple polarization splitter to give a 230 GHz channel which is always available, with simultaneous operation in the other polarization at any frequency, including possibly a second 230 GHz channel.

It would clearly be desirable to be able to operate more receivers at once. Possibilities include the use of frequency selective surfaces or materials to "drop channels", as in the various remote sensing satellites, or the use of polarizing waveplates (basically just interferometers) as at U.Mass. and the IRAM 30-metre. These are considered separately below.

Dichroic materials

There are essentially three different ways of separating channels by frequency at millimetre wavelengths:

Frequency selective surfaces (mesh filters). This is the basic filter construction used in the far infrared wavebands (see [21,22] and references therein). Some quite clever structures can be created through lithography, but the losses reported in the literature tend to be quite high (of order 30 - 50% at submm wavelengths[23]) which implies a large contribution to the receiver noise temperature. Part of this loss doubtless arises because it is not possible to create purely capacitive structures without a dielectric substrate, but it also seems that there is considerable room for improvement in the theory as well as in the construction techniques.

Multisection dielectric filters There is not a lot of information in the microwave and FIR literature about these, although the basic principles are well known from optical work and also from microwave filter synthesis techniques. The basic problem is the lack of low-loss dielectrics of a range of refractive indices, which severely limits the responses which can be synthesized: Derek Martin has recently reported results with silicon/silica(quartz)/air dielectrics, while the PTFE/quartz/air combination is probably also useful. Filters based on quarter-wave sections all tend to have spurious responses at the third harmonic which may be troublesome.

Metallic "hole-plate" The basic reference on this material seems to be the work done at JPL by Chen[24]. Things to note about this material are, first, that it acts only as a *high pass* filter; second, that the sharpness of the cutoff increases with the thickness; and third, that the sharper the cutoff the more ripple there is in the passband - possibly up to 5 or 10% for realistic parameters.

Interferometric techniques

The reflective polarizing interferometer[25] or RPI, has to my knowledge been used to separate frequency channels only at IRAM (FCRAO also use one as a LO multiplexer in the 3 mm array receiver). This may be used with or without a dielectric filling — with just an airgap it functions as a Martin-Puplett (polarizing Michelson) interferometer, but the addition of the dielectric turns it into a multibeam interferometer with a Fabry-Perot type response.

The simple MPI type response is clearly only useful in the context of frequency band diplexing when there is a harmonic relationship between the band center frequencies. With the addition of a dielectric filling the device can be tuned for a single relatively narrow band, with a broad band response in the other polarization, but the return loss for the narrow band is necessarily non-zero in this case (analogous to a FPI passband). One almost workable configuration might be to center the narrow band response of a dielectric filled RPI at about 230 GHz, for which the higher frequency bands *except* 690 GHz could all be made to have very low return losses — the return loss in the 230 GHz band would be non-negligible however, and probably of order 0.5 – 1dB to give a low enough return loss in the other polarization at 345 GHz.

Alternatively by designing the RPI to be *tunable*, and thus capable of operating on say *either* the 2^{nd} or 3^{rd} order transmission at 230 GHz it is clear that almost any other desired frequency could be brought into the passband. The same thing is probably true also of a simple MPI of course, although it might be necessary to go to higher-order maxima to get adequate response at both frequencies.

6 Holography at centimetre wavelengths

The suggestion has been made that it may be possible to align the surface using the 10.7 GHz beacon on a suitable satellite as a source of plane-wave illumination. Apart from any questions

Figure 11: *Aperture plane amplitude and phase patterns for gaussian feeds. The geometric edge of the aperture is indicated by the vertical bar at the left hand end of the phase-axis: in each case the bar indicates* $\pm 10°$ *in phase. (a) Proposed CfA antenna,* $\lambda = 28\,\mathrm{mm}$. *(b) JCMT (*$15\,\mathrm{m}$, $f/12$*),* $\lambda = 3.2\,\mathrm{mm}$. *(c) Proposed CfA antenna,* $\lambda = 28\,\mathrm{mm}$, *including a* $50\,\mathrm{mm}$ *central blockage in the subreflector.*

of whether it will actually be possible to measure phase to the necessary accuracy (of order $0.1°$), there is the question of how the antenna will perform at such long wavelengths. The most obvious problem is that of subreflector diffraction, since at a wavelength $\lambda = 28\,\mathrm{mm}$ the subreflector of the proposed baseline system is only 16λ in diameter.

I have used Anthony Lasenby's program EDGEDIFF to calculate the primary illumination function for the baseline design operating at this wavelength: amplitude and phase plots for a single radial section are shown in Figure11 (because of the way the program is implemented the calculated distribution is necessarily circularly symmetric, although this may not be exactly true). Also shown are the corresponding curves for the JCMT ($D = 15\,\mathrm{m}$; $D_s = 750\,\mathrm{mm}$) operating at a wavelength of $\lambda = 3.2\,\mathrm{mm}$ (the JCMT has a $50\,\mathrm{mm}$ hole in the centre of the subreflector, but this has been excluded from the calculation to show the underlying structure more clearly). Note that the decrease in amplitude at $\theta = 180°$ in Figure11(b) is the result of interference between the direct specular path and the signal diffracted from the edge of the subreflector.

Also shown on both plots are the zero phase levels, with $\pm 10°$ "error bars" marking the edge of the primary mirror. One problem is immediately obvious: whilst for the JCMT case the phase variations due to the secondary diffraction pattern amount to at most a few degrees (equivalent to a couple of tens of degrees at the highest observing frequency), the phase perturbation for the CfA antennas operated at $10.7\,\mathrm{GHz}$ is already $10 - 20°$, amounting to several turns at the observing frequency. Thus in order to set the surface accurately to within say $0.1°$ we require a very high level of confidence in both the measurement *and* the modelling. It may be better to reserve this low frequency measurement for an initial setting up procedure, and/or to operate the antennas from prime focus for such measurements.

7 Increasing the aperture efficiency

In principal there seem to be two main ways to go in the pursuit of higher aperture efficiency than can be obtained using a simple feed system. The first is to shape the surfaces of the primary and secondary reflectors to redistribute the feed energy toward the outer part of the dish[12],[13], thus matching the aperture fields better to the incoming radiation (which is distributed uniformly across the aperture). The second method is to modify the feed pattern itself

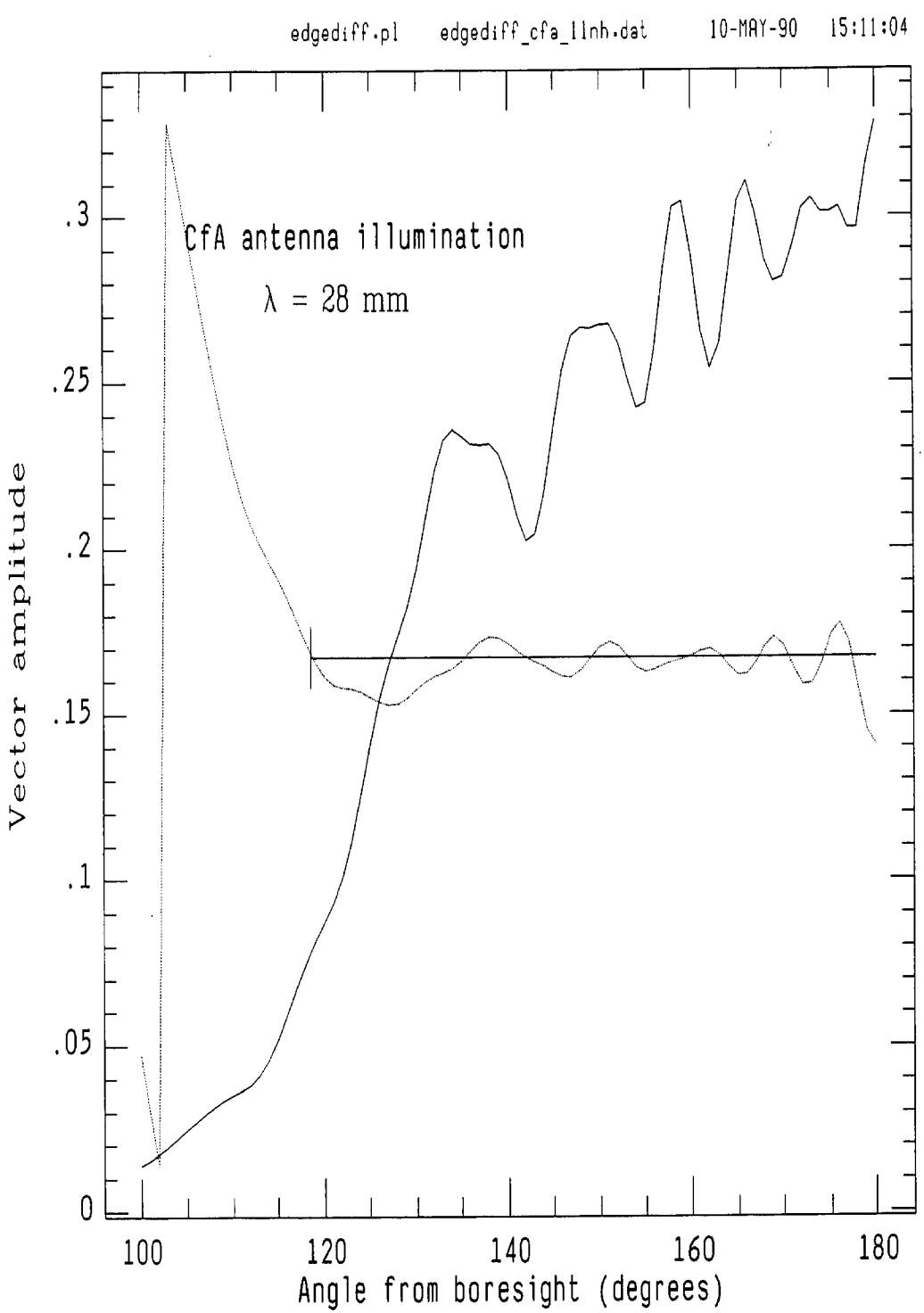
edgediff.pl edgediff_cfa_llnh.dat 10-MAY-90 15:11:04
CfA antenna illumination
λ = 28 mm
Vector amplitude
0
.05
.1
.15
.2
.25
.3
100
120
140
160
180
Angle from boresight (degrees)

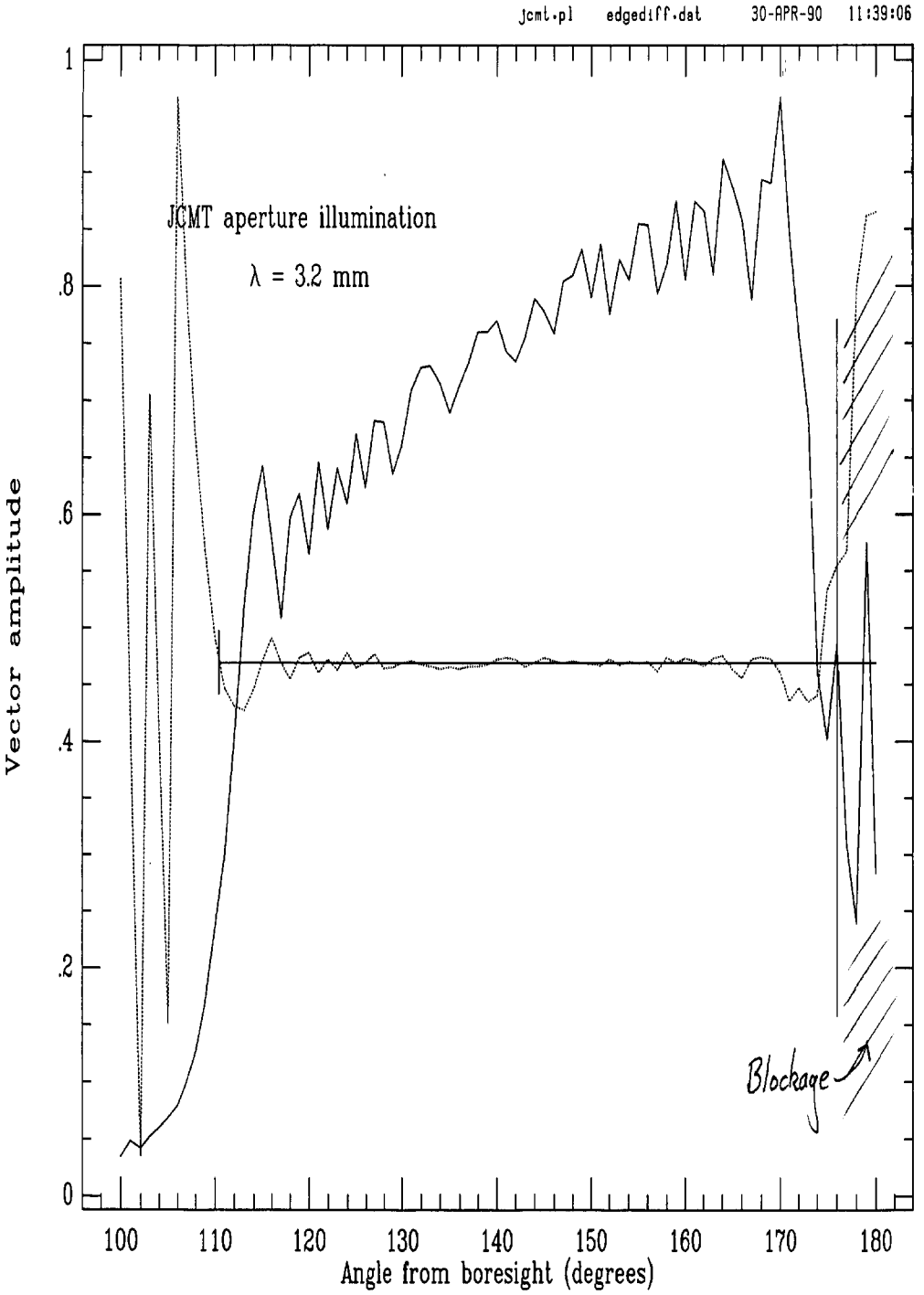
jcmt.pl edgediff.dat 30-APR-90 11:39:06
JCMT aperture illumination
λ = 3.2 mm
Vector amplitude
1
.8
.6
.4
.2
0
100
110
120
130
140
150
160
170
180
Angle from boresight (degrees)
Blockage

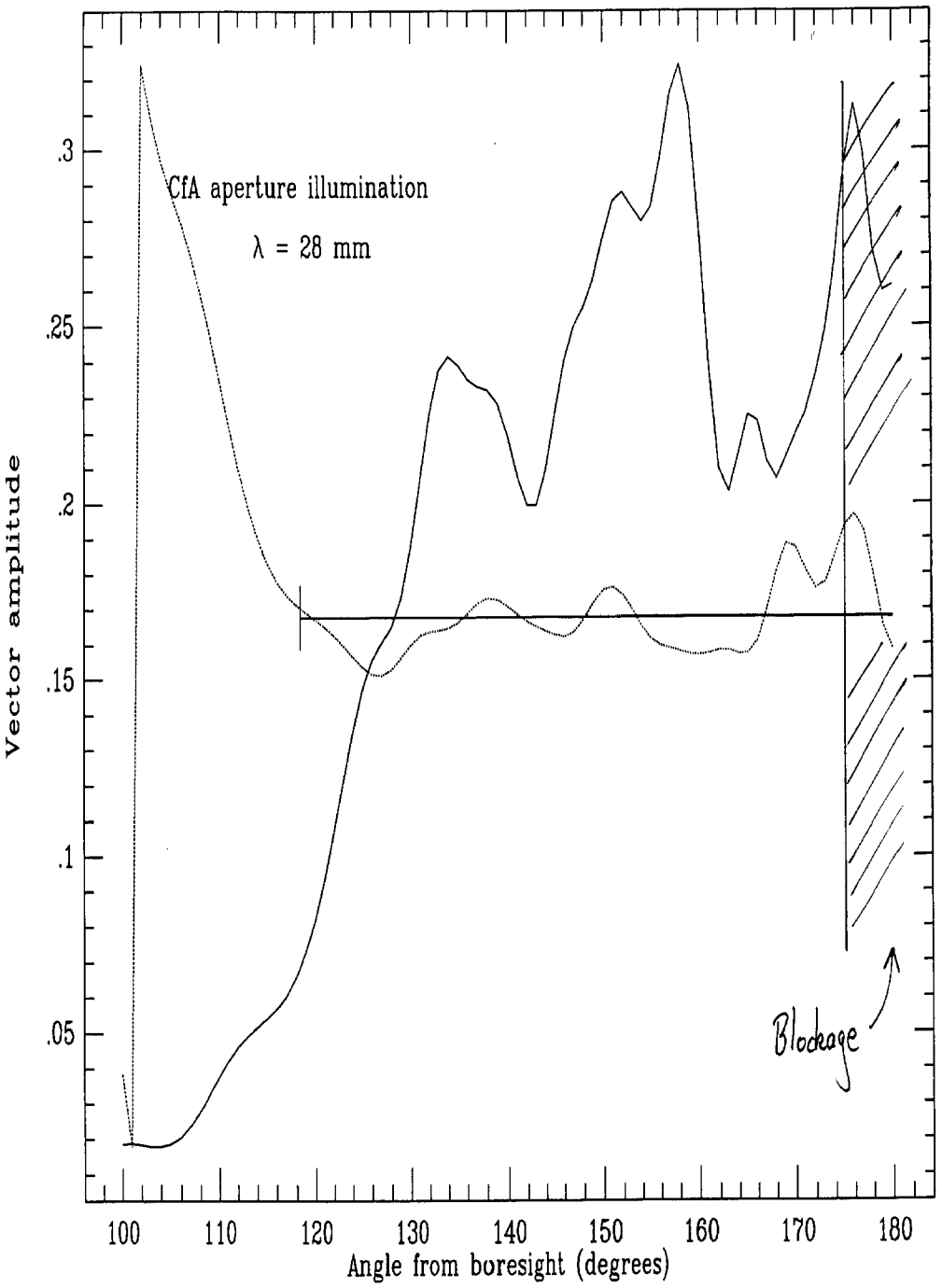
CfA aperture illumination
λ = 28 mm
Vector amplitude
.3
.25
.2
.15
.1
.05
100
110
120
130
140
150
160
170
180
Angle from boresight (degrees)
Blockage

to put the energy on the dish at the right place. To my knowledge, while the first technique has been used regularly in antennas for radioastronomy (for example in the 13 m antennas of the Cambridge 5 km telescope, and later the 25 m antennas of the VLA), the second, although widely discussed has only been applied at Hat Creek[14]: good results were reported in the literature, but apparently the system is somewhat unstable, and so is only used when maximum gain on a point source is an overriding consideration.

What efficiency can be attained with a simple (unshaped) Cassegrain system without shaping the feed illumination? For an antenna having $F/D \gg 1$ the space attenuation factor is negligible, and focal region fields due to plane wave illumination of the aperture are very close to the nominal Airy pattern. For the zero-blockage case there are analytical solutions which maximize the coupling to TE_{11} (smooth conical) and HE_{11} (scalar or hybrid-mode) feeds[15],[16]. For the scalar feed the coupling is 86.9% when the feed is placed at an image of the aperture plane, and 83.3% when the feed is placed at an image of the sky (this compares with the nominal 81.5%, regardless of focus, to be obtained with a purely gaussian illumination under the same circumstances otherwise). In order to obtain the higher figure we require some form of tertiary optics, which must be large enough to pass the higher order modes of interest: an efficiency in excess of 86% will be obtained as long as the $p = 3$ mode can pass relatively unattenuated.

Since the efficiencies quoted in the preceding paragraph are the direct coupling between normalized focal-region and horn aperture field distributions, they necessarily factor in the spillover efficiency, although blockage losses are *not* included.

These coupling efficiencies decrease when blockage is taken into account, typically by 1-2% for a central blockage equal to 10% of the primary mirror diameter, with a similar degradation being caused by the subreflector supports in a typical system. Since the spillover efficiency is already included here, it suggests that for systems with small blockages there is not a whole lot to be gained unless the effective feed edge taper can be reduced below the common value of about 10% (which, for a gaussian beam, gives a spillover efficiency alone of 90%). For the CfA baseline antenna the ratio of effective to unblocked geometric areas for the antenna is already over 90% with a 10 dB edge taper (90% spillover efficiency). Thus in order to generate a really useful improvement in gain (greater than 10%), the shaped system must be designed for much lower values of spillover — values between 1% (20dB edge taper) and 2% (17dB edge taper) are commonly used in such applications.

7.1 Shaping the antenna

As noted, this has been the option most often pursued. In principle, as the electrical size of the antenna becomes bigger, this gets easier to do, as subreflector diffraction effects *etc.* are reduced. Against this there are two main drawbacks. First, the positional tolerances become much tighter, due mainly to the increased amplitude on the outer parts of the dish, where the phase errors are generally greatest for most simple distortions. I tried playing with a published shaped antenna design[17] but was unable to duplicate the aperture phase distribution reported in that reference, so have not looked in detail at questions of sensitivity to positional errors.

However one can make a plausible case that to first order the losses are dependent only on the final illumination pattern, and *not* on the methods by which it is produced, so that the results obtained for a uniform feed illumination are probably indicative of those pertaining in this case too (see next section).

As noted above, the spillover loss is usually reduced in such systems by narrowing the feed illumination pattern to put more energy on the subreflector. Shaped antenna designs typically aim for spillover loss between 1 and 2% (17-20 dB edge taper). It is probably not possible to reduce spillover loss much below this level, as the curvature of the secondary mirror would then be reduced so much that the positional tolerances would be greatly reduced, while the the blockage losses would also become unacceptable. Even at this level the performance becomes more dependent on the feed illumination pattern being similar at all frequencies. Although this can probably be guaranteed in the microwave region it is less clear that this will be possible in the submillimeter spectral region.

The off-axis response of a shaped system deteriorates much faster than that of a traditional Cassegrain telescope[17], so that the maximum field of view will only be a few beamwidths in diameter. If the use of focal plane array detectors were being considered this would rule out the use of "common" shaped optics for this reason alone. Similarly, such shaping is inimical to the provision of a "clean" beamswitch, where both ON and OFF beams have similar and high efficiencies, unless the switch amplitude is made very small.

A further concern is the effect of the shaping on homology. R.E.Hills & A.Battilana (*priv. comm.*) have convinced themselves that homology does still work in the case of a shaped antenna system, although it is generally necessary to tilt the secondary mirror as well as translate it to compensate for the change in shape.

Unfortunately I cannot see any good way to investigate the likely increase in efficiency to be obtained with shaping by using simple geometrical optics programs. Since it is possible to obtain 100% illumination efficiency in the G.O. limit, it follows that the actual losses will be mostly due to diffraction and aperture phase errors resulting from positioning errors. To summarize then, in the absence of further information I would guess that it should be possible to obtain an illumination efficiency of up to 95% for the CfA antennas in wavebands for which corrugated feeds can be manufactured, which can be compared with the value of 87% for a simple scalar feed alone, but with the particular costs of:

- Reduced field of view (maybe not important).
- Greater dependence on the feed radiation pattern being identical at all frequencies.
- Increased sensitivity to positional errors.
- Some complication in the homology servo.
- Loss of performance at prime focus.

7.2 Shaped feed patterns

Again, there are two ways of doing this: either a single system, common to all receivers, can be installed on the secondary mirror side of the focal plane, or individual feeds can be tailored for the desired illumination. There is little difference in principle between the "common" shaped optics of the former case and the shaped reflectors: both systems suffer from similar disadvantages, although higher gains can probably be achieved in the shaped reflector system, just because of the greater size of the optical elements involved.

As noted earlier, the only working example of tertiary shaping optics for radiastronomical applications is Hudson's shaped lens[14] — this yielded a 15-20% increase in overall aperture efficiency (from $\sim$ 63% to $\sim$ 81% at 80 GHz for an antenna very similar to the CfA baseline design). At higher frequencies it is likely that lens-based designs will become too lossy, and that a design using two reflecting surfaces (as required to give adjustment of both amplitude *and* phase) may give better performance. In principle however the second solution — separate shaping for each feed — would seem to be preferred, as it does not suffer from the drawbacks associated with common shaping optics.

In order to achieve wide bandwidths with such a system we require that the shaping take place at an image of the aperture, where the fields have no phase reversals and are frequency-independent. This is in effect what the shaped antenna does: the shaping all takes place in the far field of the focal plane, where the wavefront propagates essentially according to G.O. The tertiary optics must therefore be large enough to admit all the diffraction sidelobes of the focal plane image of the uniform aperture. Inspection of the focal region Gauss-Laguerre mode coefficients in table 1 of [15] shows that modes up to $p = 6$ are required even to give 92% efficiency, so that the stops in the vicinity of the focal plane need to admit roughly 10 beam-waist radii (compared with the traditional value of 4 for single-mode optics, and 6 to achieve high efficiency with a simple horn feed). (The same result can be seen by integrating up the energy contained in successive sidelobes of the focal plane Airy pattern). For the $f/10$ optics of the baseline antenna, the beam waist is roughly 8.3 mm at λ1.3 mm, and a curved tertiary mirror would then need to be at least 85 mm in diameter.

Since there are at least 3 additional optical surfaces, care is necessary to ensure that the losses do not outweigh the gains: as noted, at submm wavelengths probably all additional elements need to be mirrors, although a dewar window may usefully double as a lens. Mirrors will necessarily be off-axis (unless some sort of cassegrain feed system is used), and need to have a relatively high f/d to reduce off-axis cross-polarization and distortion losses to an acceptable level[18].

My own guess would be that it should be possible to get the *illumination* efficiency (i.e. excluding blockage and shadowing losses, but including spillover) up to a little over 90% using this technique, with careful design, but with some cost in the overall complexity of the optical system. On the other hand, if it doesn't work or causes problems it is somewhat easier to fix this than to replace the panels!

8 Surface error specification

As shown in the Appendix, the first order loss of gain due to phase errors may be written as $G/G_0 = 1 - \overline{\delta^2}$, where $\delta(r,\phi)$ is the *total* phase error at any point (r,ϕ) in the aperture (assuming that the mean phase error about the desired distribution is zero). The calculation of $\overline{\delta^2}$ is assumed to be weighted by the aperture amplitude, $g(r,\phi)$, so in principle, if the illumination were to be gaussian, it would be possible to specify the surface errors more loosely for the outer parts of the antenna aperture. Given the gains to be obtained from a more even illumination of the aperture however, it would seem that the sensible course to follow would be to specify the errors as for uniform illumination.

There is some debate as to whether the errors should be specified normal to the aperture, normal to the panels, or in some other direction: it is the optical path length errors that matter however, and this is how the surface really ought to be specified. What we are doing is equivalent to the calculation of the aberration function for deterministic errors - we assume ray propagation along the nominal paths and then just ask the question 'How much additional phase is added by a small perturbation to the surface?'. Using this approach it can be seen that errors normal to the surface in the vicinity of the vertex enter with a simple factor of $4\pi/\lambda$ (to account for the increase in length of both incident and reflected rays), while at a radius r, where the incidence is off-normal, there is an *additional* factor of $\cos(\theta)$, where θ is the angle between the incident ray and the surface normal: for a paraboloid $\tan\theta(r) = (r/2f)$.

Thus the fractional loss of gain, $L_{Ruze} = 1 - G/G_0$ is given by:

$$\overline{\delta^2(r,\phi)} = \frac{\int_0^{2\pi}\int_{D_s/2}^{D/2} g(r,\phi)(4\pi\Delta/\lambda)^2[(1+(r/2f_1)^2]^{-1}\, r\, dr\, d\phi}{\int_0^{2\pi}\int_{D_s/2}^{D/2} g(r,\phi)\, r\, dr\, d\phi}, \tag{34}$$

where Δ is the *measured surface error in the direction of the surface normal.* For either a shaped antenna *or* a shaped illumination $f(r,\phi)$ ideally goes to unity everywhere over the aperture and drops out of the equation, and this is probably the appropriate weighting function to be used when specifying the panel accuracy.

Note that for this purpose it is irrelevant what the correlation length of any such errors is: the formula refers merely to the loss of gain in the nominal boresight direction, and as such does not tell us anything about whether the scattered energy will reappear close to the main beam (for large scale errors) or in an extended "error pattern" (as for very small scale irregularities).

9 Conclusions and areas for further study

9.1 Conclusions

I should say first that I have *not* considered the issue of an off-axis structure. Although these have many advantages for applications in communications where beam and polarization purity

are of the essence, the additional complications in design and structural analysis are many, while my understanding when I commenced this work was that the project was already committed to a 6-metre class Cassegrain antenna fundamentally similar to the BIMA design.

Throughout the report I have tried to present the material in such a way as to allow you to make your own informed choices about the development of the telescope optical design. Nonetheless I do have some fairly firm opinions of my own about how this should go, with which you are free to disagree:

1. *The optical design should be kept as simple as possible.* There are a lot of fancy features which are superfically attractive, such as beam-switching with a wobbler and the ability to multiplex several frequencies and/or polarizations at once. In my opinion the technology of mm-wave mirrors and diplexers is such that in a system of any complexity the additional losses will be *significant*, while the projected sensitivity of the system is already a worry.

2. *The primary and secondary reflectors should* not *be shaped.* Shaping imposes too many constraints on the use which may be made of the antennas at a later time, affecting everything from feeds to the potential use of imaging arrays and the utility of the beamswitch system.

3. *The beamswitch should consist of a simple focal-plane chopper with both beams located symmetrically off-axis.* The extra complexity of a full wobbler is simply not worth it, while the additional reflections are bound to introduce additional aperture phase errors.

4. *Frequency multiplexing should either be limited to simple polarization splitting, possibly with an additional reflective interferometer in the main channel to split frequencies once more.* After a non-exhaustive search I have been unable to find any dichroic material operating at these wavelengths which has simultaneously a low enough loss and a high enough bandwidth. The minimum conditions can be satisfied with a 230 GHz channel in one polarization, and additional channels for *all* wavebands (including 230 GHz) selected by a turret in the other polarization. If a reflective interferometer is used it should be dielectric filled and tunable to allow optimum transmission in the second channel.

5. *The receiver package should include a HeNe or other visible laser co-aligned to the radio beam.* This has proved to be useful on the various JCMT receivers for aligning the optics, and I think would be essential if either the Nasmyth or Coude focus is adopted.

9.2 Areas for further study

I list below areas where I really have not had time to do anything.

1. Gain with multimode feed.

2. Cross polarization levels with TE11 feeds, corner-cubes?

3. Look at effect of blockage and shadowing by struts, panel gaps, secondary mirror, etc on overall gain and performance.

4. Likely level of ohmic losses in the surface.

5. Actual layout of receiver cabin optics.

6. VSWR of proposed system

None of these seem to be very pressing, in that they do not have (except for item 3) any major implications for the design of the antenna itself, although it may be worth thinking a little bit about the ohmic losses in the reflectors, just in case (since Aluminium surfaces are still pretty good well into the optical waveband there would seem to be no need for worry however!) The effects of blockage and shadowing are well enough understood in fact, and one would always expect the antenna to be designed in such a way that the minimum losses due to these two affects are achieved that are still commensurate with the required structural rigidity, and there is plenty of evidence (*e.g.* from BIMA) that satisfactory designs already exist.

Equally, I do not expect VSWR to be a problem with this system (since the magnitude of the reflection coefficient scales with either λ or λ^2 depending on the precise details and ray path), and standing waves are less of a problem for interferometers anyway. It may be worth checking it out though, and if necessary I have quite a lot of data about these effects that could be dug out.

ACKNOWLEDGEMENTS

It is a pleasure to thank Richard Hills, Colin Masson, Buddy Martin and Anthony Murphy for many conversations and references which have helped to clarify my ideas on many of the subjects treated herein. Anthony Lasenby kindly allowed me to use his program EDGEDIFF for the holography study, and gave me much good advice on its use. I also thank the entire SMA team for making my stay in Cambridge (Mass.) so pleasant and rewarding.

REFERENCES

1. Ruze, J. 1969. *Small displacements in parabolic reflectors*, M.I.T. Lincoln Lab. unpublished report.

2. *Ruze, J, 1965. *IEEE Trans. Antennas & Propagat.* **AP-13** 660

3. *Lo, Y. T. 1960. *IRE Trans. Antennas & Propagat.* **AP-8** 347

4. Lamb, J. W. 1984. *Gain loss due to chopping secondary*, JCMT technical note ASR/MT/T/595/JL(84).

5. *Thomas, B. MacA., 1976. *Electron. Lett.* **12** 218

6. Silver, S (ed), 1965. *Microwave Antenna Theory and Design*, N.Y., Dover p423

7. Bignell, R. C. in *Synthesis mapping,* Proceedings of the NRAO VLA workshop, held in Socorro, NM, June 1982 (p 6-21)

8. *Chu, T-S, & Turrin, R. H. 1973. *IEEE Trans. Antennas & Propagat.* **AP-21** 339

9. *Kauffman, J. F., Crosswell, W. F. & Jowers, L. J., 1976. *IEEE Trans. Antennas & Propagat.*, **AP-24** 53

10. *Hannan, P. W., 1961. *IRE Trans. Antennas & Propagat.*, **AP-9** 140

11. *Jones, E. M. T., 1954, *IRE Trans. Antennas & Propagat.* **AP-2** 119

12. *Galindo, V., 1964, *IEEE Trans. Antennas & Propagat.* **AP-12** 403

13. *Williams, W. F., 1965, *Microwave J.* **8** 79

14. Hudson, J. A., Plambeck, R. & Welch, W. J., 1987. *Radio Science* **22** 1091

15. Padman, R., Murphy, J. A. & Hills, R. E., 1987. *IEEE Trans. Antennas & Propagat.* **AP-35** 1093

16. Murphy, J. A., 1988. *IEEE Trans. Antennas & Propagat.* **AP-36**, 570

17. Hudson, J. A., 1989. *Radio Science* **24** 417

18. Murphy, J. A., 1987. *International J. Infrared & Millimeter Waves* **8**, 1165

19. Murphy, J. A. & Padman, R. 1988. *International J. Infrared & Millimeter Waves* **9**, 667

20. Wood, P. J. 1980. *Reflector antenna analysis and design*, Peter Peregrinus, London. p120 and Figure 5.15

21. Timusk, T. & Richards, P.L. 1981. *Applied Optics* **20**. 1355

22. Davis, J.E. 1980, *Infrared Physics*, **20**, 287

23. Cunningham, C.T. 1983. *Infrared Physics*, **23**. 207

24. Chen, C. 1973. *IEEE Trans. Microwave Theory & Techniques*, **MTT-21**, 1

25. Erickson, N. R., 1987 *International J. Infrared & Millimetre Waves*, **8**, 1015

* These papers may be found in the IEEE press book of selected reprints, *Reflector Antennas*, edited by A.W.Love.

A Program BEAM2

In order to study the effects of feed and secondary mirror offsets, and of secondary mirror rotations, on the co- and cross-polar radiation patterns and gain of the antennas, I have written FORTRAN program, BEAM2, which runs on any VAX. With a little adaptation it should also run on any other machine supporting standard FORTRAN 77.

BEAM2 works by first locating, for each point on a mesh covering the primary reflector, the specular point on the secondary mirror for a ray emanating from the feed — it does this by applying Fermat's principle and searching for a local minimum in the total path from feed → secondary mirror → primary mirror → aperture plane, where it is assumed that the reflected ray from the primary mirror makes such a small angle with the reflector axis that the angle can be ignored in calculations of the path (this is the assumption that the reflector currents project onto the aperture plane[9], and should be applicable for any large reflector). The phase of the aperture fields at these (x, y) coordinates, is then, by definition, equal to the negative of the minimum path, although we subtract the nominal path from all measurements as a matter of computational convenience.

The amplitude of the aperture fields is assumed to be determined by the feed illumination pattern (with a suitable $\cos^2\theta/2$ space loss term), while the vector direction is now found by propagating the feed polarization vector along the already computed path. This gives us both the co- and cross-polar complex aperture field distributions, which can then be Fourier transformed to yield the far-field beam patterns. Since the location of the specular point on the secondary mirror is known it is easy to take account of any spillover arising from tilt or translation of the secondary mirror, while I also include the effect of subreflector blockage.

A.1 Geometry

I use an (x, y, z) Cartesian coordinate system, with the origin at the prime focus and z-axis pointing out along the boresight direction. Thus the general ray propagates from the feed, at $(0, 0, -2c)$, to the secondary, at (x_s, y_s, z_s), to the primary at (x_p, y_p, z_p) to the aperture plane at (x_p, y_p, z_A), with $z_A = (x_p^2 + y_p^2)/4f_1$.

The secondary mirror is assumed to be translated by a vector (x_0, y_0, z_0) and rotated about the origin by an angle α in the $x - z$ plane. The equation for the secondary mirror surface in this shifted rotated coordinate system is simply $(\frac{z''+c}{a})^2 - (\frac{x''^2+y''^2}{b^2}) = 1$, which transforms to the original (x, y, z) system using:

$$\begin{bmatrix} x'' \\ y'' \\ z'' \end{bmatrix} = \begin{bmatrix} \cos\alpha & 0 & \sin\alpha \\ 0 & 1 & 0 \\ -\sin\alpha & 0 & \cos\alpha \end{bmatrix} \cdot \begin{bmatrix} x \\ y \\ z \end{bmatrix} + \begin{bmatrix} x_0 \\ y_0 \\ z_0 \end{bmatrix} \tag{35}$$

Given values of x & y this reduces to a simple quadratic equation in z;

$$d_1 z^2 + d_2 z + d_3 = 0, \tag{36}$$

where:

$$\begin{aligned} d_1 &= c_5, \\ d_2 &= c_4 + c_3 x, \\ d_3 &= (c_1 x + c_2)x + (c_7 y + c_8)y + c_6, \end{aligned}$$

and

$$\begin{aligned} c_1 &= \frac{\sin^2\alpha}{a^2} - \frac{\cos^2\alpha}{b^2}, \\ c_2 &= -2[\frac{(c+z_0)\sin\alpha}{a^2} + \frac{x_0\cos\alpha}{b^2}], \\ c_3 &= -2\sin\alpha\cos\alpha[1/a^2 + 1/b^2], \\ c_4 &= \frac{2(c+z_0)\cos\alpha}{a^2} - \frac{2x_0\sin\alpha}{b^2}, \\ c_5 &= \cos^2\alpha/a^2 - \sin^2\alpha/b^2, \\ c_6 &= (\frac{z_0+c}{a})^2 - \frac{x_0^2+y_0^2}{b^2}, \\ c_7 &= -1/b^2, \\ c_8 &= -2y_0/b^2. \end{aligned}$$

For any given position in the aperture, (x_p, y_p, z_p), the specular point is found by searching in (x_s, y_s) for the local minimum of the total path, $P = d(FS) + d(SP) + d(PA)$. Since the minimum must be locally quadratic, and we are dealing only with small pertubations from the true paraboloid/hyperboloid geometry, it is efficient to seek the minimum using a Newton's method minimization. That is, for a general cost function P, we define the gradient and Hessian as:

$$\begin{aligned} \nabla P &= (\frac{\partial P}{\partial x})\mathbf{i} + (\frac{\partial P}{\partial y})\mathbf{j} \\ \mathbf{H} &= \begin{bmatrix} \frac{\partial^2 P}{\partial x^2} & \frac{\partial^2 P}{\partial x \partial y} \\ \frac{\partial^2 P}{\partial y \partial x} & \frac{\partial^2 P}{\partial y^2} \end{bmatrix} \end{aligned} \tag{37}$$

The new estimate of $\hat{\mathbf{x}}$ is then given by:

$$\hat{\mathbf{x}} = \mathbf{x}_0 - \mathbf{H}^{-1}\nabla P. \tag{38}$$

The components of ∇P and $\mathbf{H}$ are estimated by taking a 3×3 grid about the test point, and measuring the total path from feed to aperture via each in turn. Then:

$$\frac{\partial P}{\partial x} = \frac{f(x+\Delta, y) - f(x-\Delta, y)}{2\Delta}$$

$$\begin{aligned}
\frac{\partial P}{\partial y} &= \frac{f(x,y+\Delta)-f(x,y-\Delta)}{2\Delta} \\
\frac{\partial^2 P}{\partial x^2} &= \frac{f(x+\Delta,y)-2f(x,y)+f(x-\Delta,y)}{\Delta^2} \\
\frac{\partial^2 P}{\partial y^2} &= \frac{f(x,Y+\Delta)-2f(x,y)+f(x,y-\Delta)}{\Delta^2} \\
\frac{\partial^2 P}{\partial x \partial y} &= \frac{\partial^2 P}{\partial y \partial x} \\
&= \frac{f(x+\Delta,y+\Delta)-f(x+\Delta,y-\Delta)-f(x-\Delta,y+\Delta)+f(x-\Delta,y-\Delta)}{4\Delta^2}. \quad (39)
\end{aligned}$$

A.2 Aperture amplitude

The amplitude pattern is identical to that for the equivalent paraboloid[10], i.e. for a paraboloid of focal length Mf_1 fed from its focus. For a feed with (normalized) radiation pattern:

$$F(\theta) = 2(f_1/D)\sqrt{\frac{\ln T}{\pi}}\exp\{-\hat{a}\tan^2\theta\}, \quad (40)$$

where T is the edge taper (i.e. $F^2(\theta_s)/F^2(0)$), the aperture amplitude is then a function of r given by:

$$G(r) = \frac{1}{2D}\sqrt{\frac{-\ln T}{\pi}}\exp\{-\hat{a}\tan^2\theta_f\} \times \cos^2(\theta/2). \quad (41)$$

A.3 Feed polarization

The polarization vectors for small electric and magnetic dipole feeds, and for a small plane wave (Huygens) feed, are derived in [11]. That is, for an electric dipole:

$$\begin{aligned}
E(\psi,\xi) &= +\mathbf{i}(\cos^2\psi\cos^2\xi+\sin^2\xi) \\
&\quad -\mathbf{j}(\sin^2\psi\sin\xi\cos\xi) \\
&\quad +\mathbf{k}(\sin\psi\cos\psi\cos\xi),
\end{aligned}$$

for a magnetic dipole

$$\begin{aligned}
E(\psi,\xi) &= +\mathbf{i}(\cos\psi) \\
&\quad +\mathbf{k}(\sin\psi\cos\xi),
\end{aligned}$$

and for a small Huygens source, which is equal to a balanced sum of both electric and magnetic dipole sources,

$$\begin{aligned}
E(\psi,\xi) &= +\mathbf{i}(\cos^2\psi\cos^2\xi+\sin^2\xi+\cos\psi) \\
&\quad -\mathbf{j}(\sin^2\psi\sin\xi\cos\xi) \\
&\quad +\mathbf{k}(\sin\psi\cos\psi\cos\xi+\sin\psi\cos\xi). \quad (42)
\end{aligned}$$

A.4 Aperture plane polarization

Reflection at an infinitely conductive plane surface with normal $\hat{\mathbf{n}}$ satisfies the two boundary conditions:

- $\hat{\mathbf{n}} \times (\mathbf{E}_i + \mathbf{E}_r) = 0$ (E_t is zero)
- $\mathbf{E}_i.\mathbf{n} = \mathbf{E}_r.\mathbf{n}$ (E_n is continuous).

These equations may be combined to yield:

$$\mathbf{E}_r = -\mathbf{E}_i + 2(\mathbf{E}_i.\hat{\mathbf{n}})\hat{\mathbf{n}} \tag{43}$$

The normal to a surface expressed at $f(x, y, z) = const$ is easily derived as $\mathbf{n} \propto \pm\nabla f$. For the paraboloid then we have

$$\mathbf{n}_p \propto (-\frac{x}{2f_1}, -\frac{y}{2f_1}, 1), \tag{44}$$

while for the hyperboloid in its own frame of reference we find that

$$\mathbf{n}_s \propto (\frac{x''}{b^2}, \frac{y''}{b^2}, -\frac{z''+c}{a^2}). \tag{45}$$

Transforming this to the (x, y, z) frame, we then have:

$$\mathbf{n}_s = (\frac{x}{b^2}\cos\alpha, \frac{y}{b^2}, -\frac{x}{b^2}\sin\alpha - \frac{z+c}{a^2}\cos\alpha). \tag{46}$$

A.5 Gain computation

Three different figures of merit relating to the antenna gain are reported by the program. These are: the Ruze gain factor, which depends only on the phase mismatch errors across the aperture; the effective area of the antenna, expressed as a fraction of the geometrical unblocked area; and the efficiency as a fraction of that the antenna has when the feed and subreflector have their nominal positions.

The effective area of the nominal antenna is calculated semi-analytically (*i.e.* using a numerical approximation to the analytically expressed integral), while the gain of the actual antenna is calculated from the final aperture illumination, once all the spillover and cross polarization effects have been calculated. For reference, the various gain formula are given below:

Gain

The true gain, G, for any aperture distribution with amplitude $g(r,\phi)$ and phase error $\delta(r,\phi)$, can be expressed as:

$$G = \frac{4\pi}{\lambda^2} \times \frac{|\int_0^{2\pi}\int_0^1 g(r,\phi)exp\{j\delta(r,\phi)\}r\ dr\ d\phi|^2}{\int_0^{2\pi}\int_0^1 g^2(r,\phi)r\ dr\ d\phi}. \tag{47}$$

This integral is evaluated numerically on the same cartesian grid used to define the final aperture illumination. Because of the relatively course sampling usually used, and the convex curvature of the aperture boundary, the gain is systematically overestimated — for a 16×16 sampling the error may be as great as 0.7%. The gain also changes discontinuously as resolution cells are masked off to represent spillover etc. Both of these effects can be reduced by using finer sampling if it is important for the application.

Effective area

$$A_e = G\frac{\lambda^2}{4\pi}. \tag{48}$$

In this case the inner limit of integration in the radial coordinate of (47) is taken to be r_s/R_0, so as to exclude the blocked portion of the aperture from consideration. Likewise spillover is ignored in both equations by setting the outer limit to 1, rather than ∞. This definition of effective area is then such as to measure only the illumination efficiency: if the antenna is illuminated with only a small edge taper the ratio of effective area to true area returned by the program will approach 1. For the same spillover then this measures how well the antenna aperture is used.

Ruze gain

The Ruze gain is based on the small phase error approximation, and thus tends to *underestimate* the true gain when the phase error $\delta(r,\phi) \not\ll 1$. For small phase errors however, and in combination with the overall relative effective area, it is a useful indicator of the relative importance of phase and amplitude (spillover *etc.*) errors in determining the final gain.

$$\eta_{Ruze} = G/G_0 \simeq 1 - \overline{\delta^2} + (\bar{\delta})^2. \tag{49}$$

The statistics $\overline{\delta^2}$ and $(\bar{\delta})^2$ are accumulated at the same time as the aperture distribution is evaluated.

A.6 Beam pattern computation

The beam pattern is calculated from the aperture phase and amplitude using an FFT to approximate the radiation integral

$$F(\sin\theta_x, \sin\theta_y) = \int_{-\infty}^{+\infty}\int_{-\infty}^{+\infty} G(x,y)\exp\{-2\pi i\frac{x\sin\theta_x + y\sin\theta_y}{\lambda}\}\,dx\,dy \tag{50}$$

or in the small angle approximation, with $\sin\theta_x \simeq \theta_x$ and $\sin\theta_y \simeq \theta_y$,

$$F(\theta_x, \theta_y) = \int_{-\infty}^{+\infty}\int_{-\infty}^{+\infty} G(x,y)\exp\{-2\pi i\frac{x\theta_x + y\theta_y}{\lambda}\}\,dx\,dy. \tag{51}$$

Considering for the moment just the 1-dimensional problem, the FFT is an algorithm for evaluating the discrete Fourier transform of a sequence of values $\{f_1, f_2, \ldots, f_{N-1}\}$, such that:

$$F_k = \sum_{n=0}^{N-1} f(n\Delta x)\exp\{-2\pi i\frac{nk}{N}\} \tag{52}$$

which may be compared to the approximate 1-D form of (51):

$$F(\theta) = \Delta x \times \sum_{n=0}^{N-1} f_n \exp\{-2\pi i n\Delta x\frac{\theta}{\lambda}\}. \tag{53}$$

By analogy then we interpret the term G_k of the *inverse* DFT of the sequence of sampled aperture fields, $DFT^{-1}\{f_1, f_2, \ldots, f_{N-1}\}$, to be equal to $\frac{N}{D}F(k\lambda/D)$. That is, applying an inverse DFT to the sequence of aperture fields, we interpret the k^{th} term of the resulting sequence as N/D times the value of the field at a value of $\sin\theta = k\lambda/D$.

It follows that if we were to take the inverse DFT of the aperture fields directly, then the resulting beam map would have extent $N\lambda/D$, and resolution cell λ/D, which is not really what we want. In order to obtain better resolution we first interpolate, by dropping the sampled aperture into the center of a larger array, of extent N'. We also have to "chequerboard" the array, by multipliying alternate pixels by -1, before and after transforming, to shift the phase-centre of the transform to the $(N'/2+1)^{th}$ pixel. With these modifications the resolution cell is reduced to $\lambda N/N'$, while the map extent is still $N\lambda/D$

The number of resolution cells across the aperture, N, is a user-definable parameter in the range 1 to 256, with computation time for any antenna configuration scaling roughly as the square of the chosen value. The aperture distribution is always dropped into the middle of an array of size `MSIZE` × `MSIZE`, where `MSIZE` ($= N'$) is a FORTRAN parameter (default equals 256). Thus the choice of `N` determines both the accuracy of the gain determination, *and* the size of the final beam map in terms of nominal beamwidths.

The final figure (12) shows some examples of results from the program.

Figure 12: *Example radiation pattern calculations from BEAM2. In all cases the solid contours run from 0.1 to 1.0 in increments of 0.1, while the dot-dash contours are at levels of 0.025 and 0.05. (a) Co- and cross-polar radiation patterns for the CfA baseline antenna, operating at* $\lambda = 1\,\mathrm{mm}$, *with lateral shifts of the subreflector* $\Delta x_s = \Delta y_s = 1\,\mathrm{mm}$. *The coma lobe is clearly visible in the co-polar pattern. (b) Co- and cross-polar patterns for the same antenna and wavelength, with the subreflector rotated by 2° about prime focus in the* x *(elevation) direction. (c) Co- and cross-polar patterns of the same antenna, with uniform illumination.*

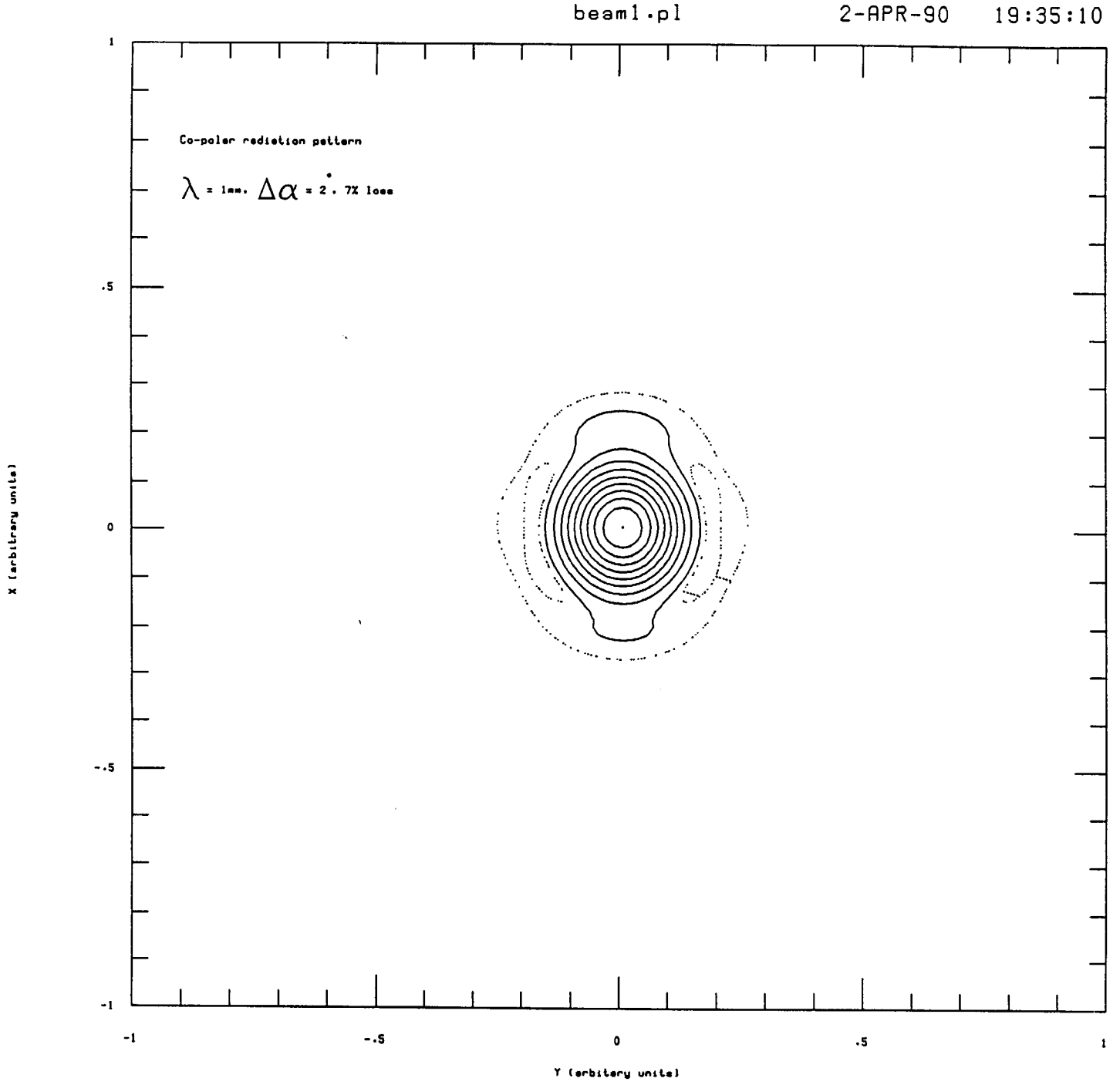
beam1.pl
2-APR-90 19:35:10
Co-polar radiation pattern
λ = 1mm. Δα = 2°. 7% loss
1
.5
0
-.5
-1
-1
-.5
0
.5
1
X (arbitrary units)
Y (arbitary units)

Fig 12b

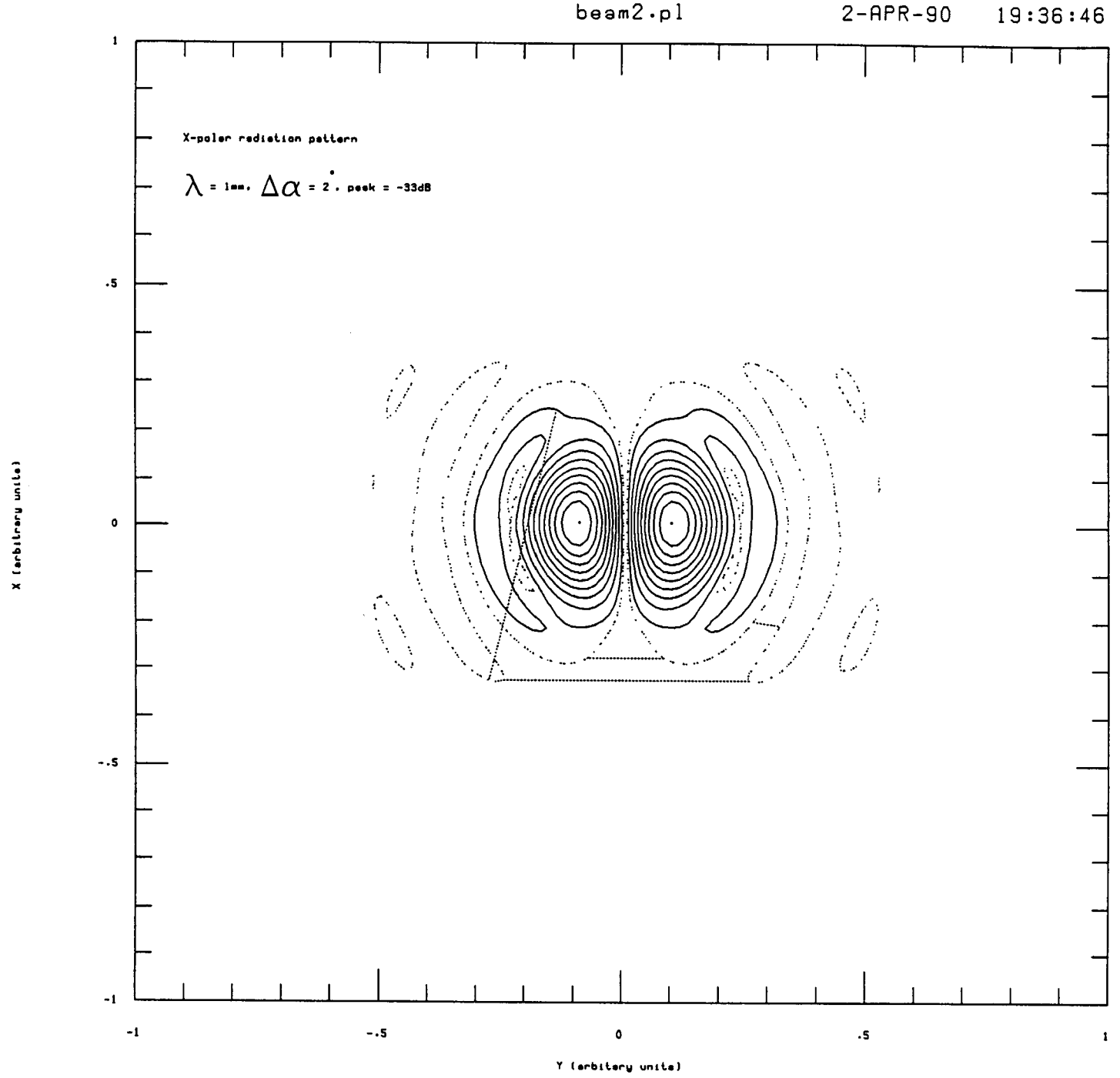
beam2.pl
2-APR-90 19:36:46
X-polar radiation pattern
λ = 1mm, Δα = 2°, peak = -33dB
X (arbitrary units)
Y (arbitary units)
1
.5
0
-.5
-1
-1
-.5
0
.5
1

Fig 12b

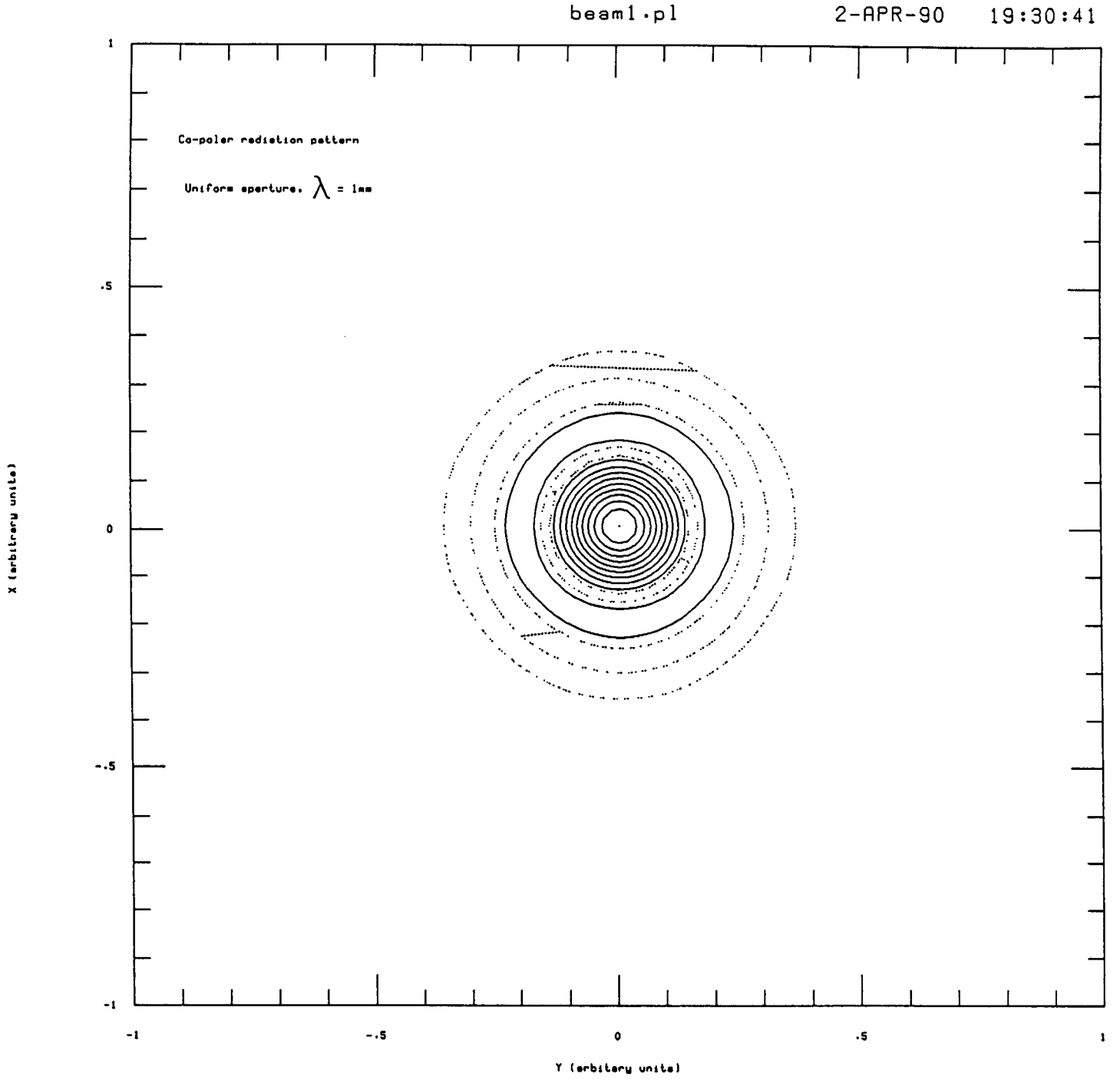
beam1.pl
2-APR-90 19:30:41
Co-polar radiation pattern
Uniform aperture, λ = 1mm
X (arbitrary units)
Y (arbitary units)
1
.5
0
-.5
-1
-1
-.5
0
.5
1

Fig 12c

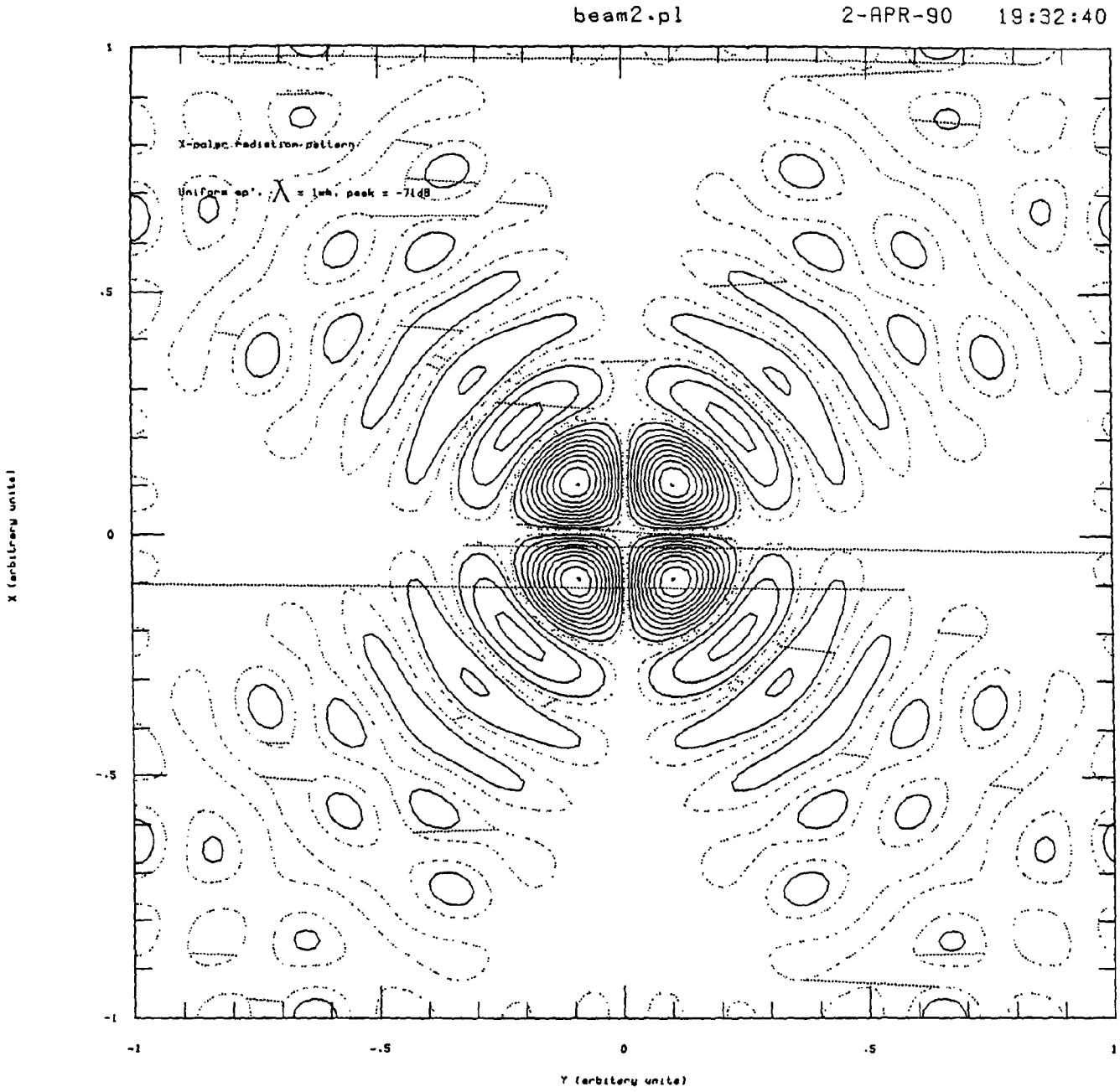
beam2.pl
2-APR-90 19:32:40
X-polar radiation pattern
Uniform ap', λ = 1wk, peak = -71dB
X (arbitrary units)
Y (arbitrary units)
1
.5
0
-.5
-1
-1
-.5
0
.5
1

Fig 12c